HSPRO Controls Early *Nicotiana attenuata* Seedling Growth during Interaction with the Fungus *Piriformospora indica*[1[C][W][OA]]

Stefan Schuck, Iris Camehl, Paola A. Gilardoni, Ralf Oelmueller, Ian T. Baldwin, and Gustavo Bonaventure*

Department of Molecular Ecology, Max Planck Institute for Chemical Ecology, Jena 07745, Germany (S.S., P.A.G., I.T.B., G.B.); and Institute of General Botany and Plant Physiology, Friedrich-Schiller University of Jena, D–07743 Jena, Germany (I.C., R.O.)

In a previous study aimed at identifying regulators of *Nicotiana attenuata* responses against chewing insects, a 26-nucleotide tag matching the *HSPRO* (*ORTHOLOG OF SUGAR BEET Hs1*$^{pro\text{-}1}$) gene was found to be strongly induced after simulated herbivory (Gilardoni et al., 2010). Here we characterized the function of *HSPRO* during biotic interactions in transgenic *N. attenuata* plants silenced in its expression (ir-*hspro*). In wild-type plants, *HSPRO* expression was not only induced during simulated herbivory but also when leaves were inoculated with *Pseudomonas syringae* pv *tomato* DC3000 and roots with the growth-promoting fungus *Piriformospora indica.* Reduced *HSPRO* expression did not affect the regulation of direct defenses against *Manduca sexta* herbivory or *P. syringae* pv *tomato* DC3000 infection rates. However, reduced *HSPRO* expression positively influenced early seedling growth during interaction with *P. indica*; fungus-colonized ir-*hspro* seedlings increased their fresh biomass by 30% compared with the wild type. Grafting experiments demonstrated that reduced *HSPRO* expression in roots was sufficient to induce differential growth promotion in both roots and shoots. This effect was accompanied by changes in the expression of 417 genes in colonized roots, most of which were metabolic genes. The lack of major differences in the metabolic profiles of ir-*hspro* and wild-type colonized roots (as analyzed by liquid chromatography time-of-flight mass spectrometry) suggested that accelerated metabolic rates were involved. We conclude that *HSPRO* participates in a whole-plant change in growth physiology when seedlings interact with *P. indica*.

Nicotiana attenuata is a wild annual tobacco (*Nicotiana* spp.) plant native to the deserts of the southwestern United States and it germinates after fires from long-lived seed banks to form monocultures in post-fire nitrogen (N)-rich soils (Baldwin and Morse, 1994). As a result of its life history, *N. attenuata* grows rapidly after seed germination and the control of seedling growth is critical for plant fitness since young seedlings are more vulnerable to environmental stresses. In addition to water availability and high temperatures and light intensities, *N. attenuata* plants interact with unpredictable communities of beneficial and nonbeneficial organisms in their natural environment (Baldwin and Preston, 1999; Barazani et al., 2005; Long et al., 2010). With regard to biotic interactions, *N. attenuata* (and plants in general) readjust their metabolic and growth programs to meet the new requirements of de novo biosynthesis of direct (e.g. accumulation of toxic metabolites) and indirect (e.g. production of volatiles) defense responses as well as to induce tolerance mechanisms (e.g. carbon [C] and N bunkering in roots) or to facilitate symbiotic interactions (Rosenthal and Kotanen, 1994; Bardgett et al., 1998; Schwachtje and Baldwin, 2008). Activation of these responses requires metabolic energy and the redirection of C, N, and additional resources throughout the whole body of the plant (Schwachtje and Baldwin, 2008; Bolton, 2009). With the aim of identifying regulatory components of the pathways mediating defense and tolerance responses against lepidopteran larvae in *N. attenuata*, a serial analysis of gene expression approach was recently performed by our group to quantify the early transcriptional changes elicited by the insect elicitor *N*-linolenoyl-Glu (18:3-Glu; Gilardoni et al., 2010). The analysis targeted mRNAs encoding rare transcripts constitutively expressed and showing rapid and transient induction after 18:3-Glu elicitation. Among the approximately 500 differentially expressed transcripts, more than 25% corresponded to putative regulatory components (Gilardoni et al., 2010). One of these components was a homolog of a group of proteins denominated putative nematode resistance

[1] This work was supported by the Deutsche Forschungsgesellschaft (grant nos. BO3260/3–1 and 3–2) and the Max Planck Society.

* Corresponding author; e-mail gbonaventure@ice.mpg.de.

The author responsible for distribution of materials integral to the findings presented in this article in accordance with the policy described in the Instructions for Authors (www.plantphysiol.org) is: Gustavo Bonaventure (gbonaventure@ice.mpg.de).

[C] Some figures in this article are displayed in color online but in black and white in the print edition.

[W] The online version of this article contains Web-only data.

[OA] Open Access articles can be viewed online without a subscription.

www.plantphysiol.org/cgi/doi/10.1104/pp.112.203976

protein or ORTHOLOG OF SUGAR BEET Hs1^{pro-1} (HSPRO) based on their homology to Hs1^{pro-1} from sugar beet (*Beta vulgaris*; Cai et al., 1997).

To our knowledge, the study describing the role of Hs1^{pro-1} was the first to provide functional information for this group of proteins, and Hs1^{pro-1} was originally identified as a gene conferring resistance to the beet cyst nematode *Heterodera schachtii* (Cai et al., 1997). Subsequent studies performed in different plant species suggested however that this group of proteins has a more general role in the regulation of plant responses to biotic and abiotic stresses. For example, the Arabidopsis (*Arabidopsis thaliana*) genome encodes for two homologs of *Beta procumbens Hs1^{pro-1}*, *HSPRO1*, and *HSPRO2* and these two genes have been categorized as general stress signaling genes (Baena-González and Sheen, 2008). The expression of Arabidopsis *HSPRO* genes is not induced by nematode feeding (Puthoff et al., 2003) but it can be differentially induced by salicylic acid (SA), *Pseudomonas syringae* pv *tomato* (*Pst*) DC3000, and *Xanthomonas campestris* pv *campestris* infection, the bacterial elicitor flagellin22 (flg22), phosphate starvation, salt stress, drought, wounding, and UV-B (Hammond et al., 2003; Zipfel et al., 2004; Cominelli et al., 2005; Gissot et al., 2006; Fujita et al., 2007; Kudla et al., 2007; Murray et al., 2007; Walley et al., 2007). Genetic disruption of *HSPRO2* in Arabidopsis increased susceptibility to *Pst* DC3000 (Murray et al., 2007) and its ectopic expression confers increased resistance against oxidative stress (Luhua et al., 2008). The role of *HSPRO* genes in these processes is at present unknown. Interestingly, in Arabidopsis, it has been shown that HSPRO1 and HSPRO2 interact with the AKIN$\beta\gamma$ (adaptor-regulator related to the Suc NONFERMENTING1 [SNF1]/AMPK family) subunit of the SNF1-related protein kinase (SnRK1) complex (Gissot et al., 2006). This complex is a heterotrimeric protein kinase complex related to the *Saccharomyces cerevisiae* SNF1 kinase (Baena-González and Sheen, 2008). Plant SnRK1s are central regulators of metabolism via the control of gene expression and enzyme activity (Halford et al., 2003; Lovas et al., 2003; Schwachtje et al., 2006; Baena-González and Sheen, 2008).

In this study, we analyzed the role of the *HSPRO* gene in *N. attenuata* during diverse biotic interactions, including *M. sexta* herbivory, *Pst* DC3000 infection, and association with the growth-promoting fungus *Piriformospora indica*. *P. indica* is a root-colonizing basidiomycete of the order Sebacinales (Varma et al., 1999; Weiss et al., 2004) and is closely related to fungal clones isolated from soil samples collected from the rhizosphere of *N. attenuata* in its natural habitat (Barazani et al., 2005). *P. indica* has the ability to colonize roots of different plant species including *N. attenuata*, thereby initiating a mutualistic interaction resulting in plant growth promotion (Sahay and Varma, 1999; Barazani et al., 2005; Achatz et al., 2010; Fakhro et al., 2010). The results demonstrated that *HSPRO* is not involved in the regulation of traits associated with direct defense responses against *M. sexta* herbivory or performance of *Pst* DC3000 during infection, but is a negative regulator of *N. attenuata* early seedling growth stimulated by *P. indica*.

RESULTS

Sequence and Localization Analyses of *N. attenuata* HSPRO

From the serial analysis of gene expression analysis published recently by Gilardoni et al. (2010), a 26-nucleotide tag (UniTag-6205) was identified as a tag whose abundance was 18-fold enriched in leaves of *N. attenuata* plants within 30 min of elicitation with the fatty acid amino acid conjugate (FAC) 18:3-Glu. The full-length complementary DNA corresponding to UniTag-6205 was obtained by 5′ and 3′ RACE and it was found to encode for an open reading frame of 1,437 bases and for a predicted polypeptide of 478 amino acids (M_r: 54 kD). The protein presented 45% to 70% amino acid sequence identity to the sugar beet Hs1^{pro-1} protein and to several homologs in other plant species including HSPRO1 and HSPRO2 from Arabidopsis (Fig. 1A; Supplemental Figs. S1 and S2). For consistency with the Arabidopsis nomenclature, we named the *N. attenuata* homolog HSPRO. The phylogenetic analysis of the 21 closest homologs of HSPRO from different plant species found in GenBank showed that amino acid similarity between paralogs was higher than between orthologs, with sequences from legumes, monocotyledonous, and Arabidopsis species clustering together (Fig. 1B). Interestingly, HSPRO sequences from monocots clustered closer to sequences from the moss *Physcomitrella patens* than did to sequences from dicots (Fig. 1B), thus not following the phylogeny of the taxa shown. In silico analysis predicted cytosolic localization for HSPRO and this prediction was confirmed by expressing an HSPRO-enhanced GFP (EGFP) C-terminal fusion protein in leaf protoplasts and analysis by fluorescence microscopy (Fig. 1C).

HSPRO Expression Is Induced by Different Biotic Stress-Associated Treatments

Analysis of *HSPRO* mRNA levels in *N. attenuata* plants showed that this gene was not only differentially induced by 18:3-Glu but also by *M. sexta* and *Spodoptera exigua* oral secretions (OS) in leaves (with *M. sexta* OS being the strongest inducer: approximately 12-fold) when compared with wounding (control treatment; Fig. 2A). FAC elicitation induces a strong jasmonic acid (JA) burst in *N. attenuata* plants (Kallenbach et al., 2010) and analysis of *HSPRO* expression in plants deficient in either JA (ir-*lox3*) and JA-Ile (ir-*jar4/6*) production or JA signaling (ir-*coi1*) showed that the induction of *HSPRO* was negatively affected by JA production (i.e. increased *HSPRO* mRNA

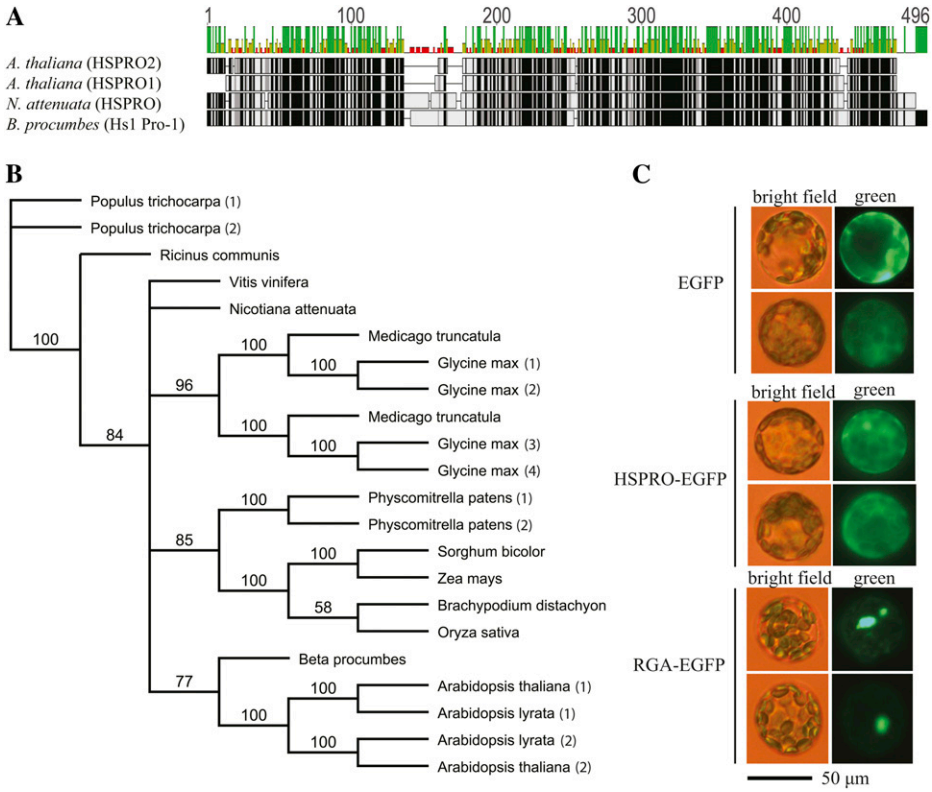

Figure 1. Analysis of HSPRO amino acid sequence and cellular localization. A, Schematic protein sequence alignment of *N. attenuata* HSPRO (JQ354963), Arabidopsis HSPRO1 (At2g4000) and HSPRO2 (At3g55840), and *B. procumbes* Hs1^{pro-1} (U79733 plus DQ148271). The cartoon above the sequences shows the percentage of similarity (green bars within the overlapping regions represent identical amino acids in the four sequences). See Supplemental Figure S2 for a detailed amino acid alignment. B, Phylogenetic analysis of HSPRO proteins from different organisms. The tree was constructed using the Geneious Pro software (5.3.4) with the Jukes-Cantor genetic distance model and the neighbor-joining tree building method with bootstrapping (602 random seed, 100 replicates, and 50% support threshold). See Supplemental Figure S1B for a reference to accession numbers. C, Arabidopsis mesophyll protoplasts were isolated and transiently transfected with vectors carrying either EGFP alone (cytosolic localization), EGFP C-terminal fusions with REPRESSOR OF ga1-3 (RGA-EGFP; nuclear localization), and EGFP C-terminal fusions with HSPRO (HSPRO-EGFP) under regulation of the cauliflower mosaic virus *35S* promoter. After transfection, protoplasts were incubated for 15 h in the dark at room temperature and images were taken with a Zeiss Axioplan fluorescence microscope with standard settings for EGFP.

accumulation in ir-*lox3* plants compared with the wild type [control]) but not affected in plants deficient in JA-Ile accumulation or *CORONATINE-INSENSITIVE1* (*COI1*) expression (Fig. 2B). Moreover, the induction of *HSPRO* expression depended on SA-induced protein kinase, a known regulator of JA-mediated responses in *N. attenuata* (Wu et al., 2007; Supplemental Fig. S3). *HSPRO* mRNA levels were induced 2.5-fold after 12 h of *Pst* DC3000 infection and 30-fold after 1 h of exogenous SA treatment (Fig. 2C; Supplemental Fig. S3) whereas they were not induced by *Agrobacterium tumefaciens* infection compared with control treatment (Fig. 2C). Thus, similar to other plant species, *HSPRO* responded to multiple biotic-stress-associated stimuli.

Analysis of tissue-specific expression showed that *HSPRO* was ubiquitously expressed with the highest levels of expression in flower parts, in particular the corolla (Fig. 2D).

Generation of *N. attenuata* Plants with Stably Reduced Levels of HSPRO Expression

To examine in further detail the function of *HSPRO*, stably transformed *N. attenuata* plants with reduced expression of this gene were generated by inverted-repeat-mediated RNA interference (see "Materials and Methods" for a detailed description of the generation of these plants). Two homozygous independently transformed lines, named ir-*hspro*1 and ir-*hspro*2, were selected and used for all the experiments described below. These lines harbored a single T-DNA insertion in their genomes (Fig. 3A) and the levels of *HSPRO* mRNA were reduced on average by 93% (ir-*hspro*1) and 95% (ir-*hspro*2) compared with wild-type plants after 18:3-Glu elicitation (a condition that maximizes *HSPRO* expression; Fig. 3B). A third line, ir-*hspro*3 harbored two T-DNA insertions in its genome (Figs. 3A) and it was used only for a selected number of

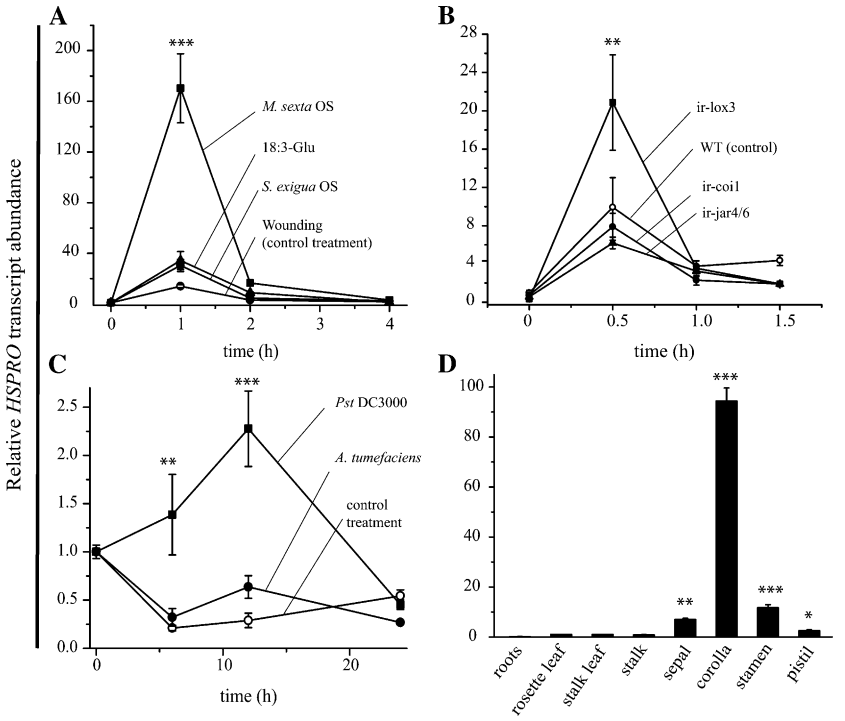

Figure 2. Analysis of *HSPRO* expression in wild-type and transgenic *N. attenuata* plants. The levels of *HSPRO* mRNA were analyzed by qPCR in leaves of wild-type and transgenic *N. attenuata* plants after different treatments and in different plant organs and tissues. mRNA levels are expressed relative to the levels of the reference gene Na-*EF1A*. Quantification was performed by the comparative cycle threshold method (n = 3–6; bars = ±SE). A, Elicitation of leaves from wild-type plants with OS from *M. sexta* and *S. exigua* larvae, synthetic 18:3-Glu, or wounding. One way-ANOVA with Tukey's post-hoc test (*M. sexta* OS versus wounding); ***, $P < 0.001$. B, Elicitation of leaves from wild-type and transgenic lines with synthetic 18:3-Glu. One way-ANOVA with Tukey's post-hoc test (ir-*lox3* versus the wild type); **, $P < 0.01$. C, Infection of leaves from wild-type plants with *Pst* DC3000 and *A. tumefaciens* (GV3101). One-way ANOVA with Tukey's post-hoc test (*Pst* DC3000 versus control); **, $P < 0.01$; ***, $P < 0.001$. D, *HSPRO* mRNA levels in different organs and tissues of wild-type *N. attenuata* plants. Relative levels of *HSPRO* mRNA in roots were set arbitrarily to 1. One-way ANOVA with Tukey's post-hoc test (roots versus other tissues); *, $P < 0.05$; **, $P < 0.01$; ***, $P < 0.001$.

experiments. The levels of *HSPRO* mRNA in this line were reduced by 91% compared with the wild type (Fig. 3B).

The growth and morphology of ir-*hspro* plants grown under standard chamber and glasshouse conditions were indistinguishable from those of the wild type at all stages of development (Fig. 3, C and D; see also below).

HSPRO Does Not Affect Defense Responses against *M. sexta* Herbivory and *Pst* DC3000 Infection

Based on the strong expression response of *HSPRO* to *M. sexta* OS and FACs (Fig. 2A), we first assessed whether ir-*hspro* plants were more susceptible to the attack of *M. sexta* larvae. The results showed that the performance of these larvae (evaluated as the gain of body mass as a function of time) was similar between ir-*hspro* and wild-type plants (Supplemental Fig. S4A). Consistently, the quantification of the JA-inducible defense metabolites nicotine, chlorogenic acid (3-*O*-caffeoylquinic acid), and rutin (quercetin-3-*O*-rutinoside) after elicitation with *M. sexta* OS showed that their amounts were similar in leaves of ir-*hspro* and wild-type plants (Supplemental Fig. S4, B–D).

Second, based on the high levels of *HSPRO* expression in flower parts and in particular the corolla (Fig. 2D), we assessed whether this gene participates in the regulation of traits (defensive and nondefensive) associated with the interaction of insects with flowers. The analyzed traits were: (1) the production of benzyl acetone in corollas, (2) the volume of nectar in flowers, (3) the amount of nicotine in nectar, (4) the amount of sugar in nectar, and (5) the level of trypsin protease inhibitor activity in ovaries and anthers. These traits were quantified in wild-type and ir-*hspro* plants grown either under control conditions or under the attack of *M. sexta* caterpillars for 15 consecutive days. All samples were collected at the end of the treatment (15 d). The results showed that the analyzed traits did not differ between ir-*hspro* and wild-type plants (Supplemental Fig. S5).

Finally, based on the induction of *HSPRO* mRNA levels by SA and *Pst* DC3000 infection (Fig. 2C), ir-*hspro* and wild-type plants were infected with this pathogen by leaf infiltration. In two independent experiments, the number of colony forming units (CFU) retrieved per area of infected leaves was similar between wild-type and ir-*hspro* plants at 24, 48, and 72 h postinfection (data not shown).

HSPRO Participates in the Mechanisms That Regulate Growth Promotion by the Fungus *P. indica*

The induction of *HSPRO* mRNA levels by diverse biotic-related stresses prompted us to investigate the interaction of ir-*hspro* plants with the growth-promoting fungus *P. indica*. This fungus has the capacity to establish symbiotic associations with roots of a broad range of plant species including *N. attenuata* (Varma et al., 1999; Barazani et al., 2005; Waller et al., 2005; Qiang et al., 2011). To study the interaction between ir-*hspro* seedlings and *P. indica*, we used a previously described plate system (Camehl et al., 2011; Fig. 4A). In this system, the hyphae reached the seedling's roots between day 4 and 5 after the start of the experiment (i.e. transfer of seedlings to plates containing *P. indica*; see "Materials and

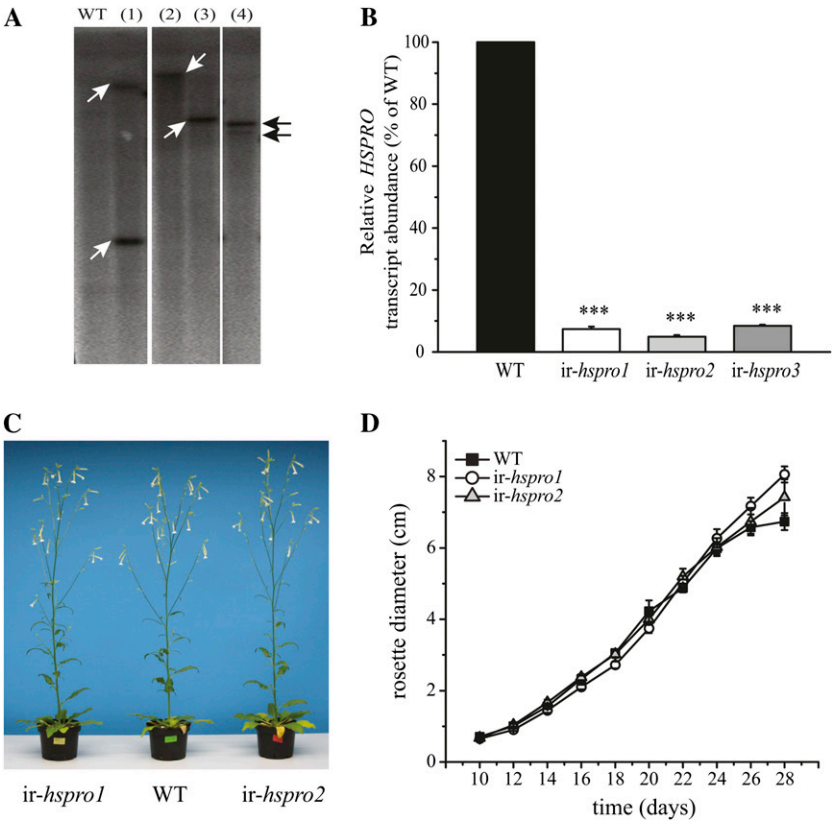

Figure 3. Characterization of ir-*hspro* plants. A, Southern-blot analysis of the ir-*hspro* transgenic lines. Genomic DNA from four independent ir-*hspro* *N. attenuata* lines (1–4) and wild-type plants was digested with *Eco*RV and resolved by agarose gel electrophoresis. A ^{32}P-labeled fragment corresponding to the hygromycin resistance gene *nptII* was used as a probe. The white arrows point to individual T-DNA insertions (lane 2: ir-*hspro1*; lane 3: ir-*hspro2*; lane 4: ir-*hspro3*). B, Analysis of *HSPRO* mRNA levels in leaves of ir-*hspro* lines at 1 h after 18:3-Glu elicitation ($n = 6$; bars = ±SE). Relative mRNA levels were quantified as detailed in caption of Figure 1. One-way ANOVA with Tukey's post-hoc test (wild type versus ir-*hspro*); ***, $P < 0.001$. C, Morphology of wild-type and ir-*hspro* plants at the late elongation stage. D, Rosette growth curve (measured as rosette diameter) of wild-type and ir-*hspro* plants (n = 8–20; bars = ±SE). [See online article for color version of this figure.]

Methods" for a detailed description of the system used). Unless noted, all the experiments were conducted with seedling tissue harvested at day 14 after the start of the experiment. In wild-type seedlings, *HSPRO* transcripts were undetected in roots of control treatment but strongly induced upon *P. indica* colonization (Fig. 4B). In colonized roots of ir-*hspro* seedlings, the level of this mRNA was also increased but it remained at less than 8% of wild-type levels (Fig. 4B).

The quantification of root, shoot, and seedling fresh biomasses showed that *P. indica*-colonized ir-*hspro* seedlings gained on average 30% more biomass than *P. indica*-colonized wild-type seedlings (Fig. 4, C–E). This experiment was repeated seven times with consistent results (Supplemental Table S1). The differential growth promotion of ir-*hspro* seedlings varied between 15% and 73% depending on the experiment and the length of the incubation period (10 or 14 d) with an average growth promotion of 32% (Supplemental Table S1). Thus, in addition to the growth promotion effect of *P. indica* observed on wild-type seedlings (Fig. 4, C–E; Supplemental Table S1), there was an enhanced differential growth promotion on ir-*hspro* seedlings. The difference in growth was maintained as the seedlings were transferred to soil and grown in the glasshouse for maturation. In this case, the rosette diameter was determined as a parameter of growth (Supplemental Fig. S6A). At the end of the rosette expansion period (i.e. start of reproductive phase [bolting]), the rosette diameter was similar between the two genotypes (Supplemental Fig. S6A). A higher percentage of ir-*hspro* plants bolted 1 d earlier than the wild type (25% and 42% of ir-*hspro1* and ir-*hspro2*, respectively) and the rate of stalk elongation and flowering time were similar between the genotypes (Supplemental Fig. S6, B–D). These results showed that the growth of *P. indica*-colonized ir-*hspro* seedlings was primarily accelerated during the early stages of seedling growth without consequences for the final plant size at the mature stage.

To analyze if the differential growth promotion of ir-*hspro* seedlings during interaction with *P. indica* was the result of a differential assimilation of CO_2 produced by the fungus, ir-*hspro* and wild-type seedlings and *P. indica* were grown together but physically separated from one another in a three-sector split-plate system (Supplemental Fig. S7A). This setting allowed for the exchange of CO_2 between organisms in the absence of physical contact. No differential growth promotion was observed between wild-type and ir-*hspro* seedlings in this experiment (Supplemental Fig. S7, B–D), indicating that physical interaction between roots and *P. indica* was required to differentially stimulate the growth of ir-*hspro* seedlings.

Analysis of *P. indica*-Root Interactions and *P. indica*-Induced Changes in Phytohormone Levels

Microscopy analysis of *P. indica*-colonized roots of wild-type and ir-*hspro* seedlings at two different times

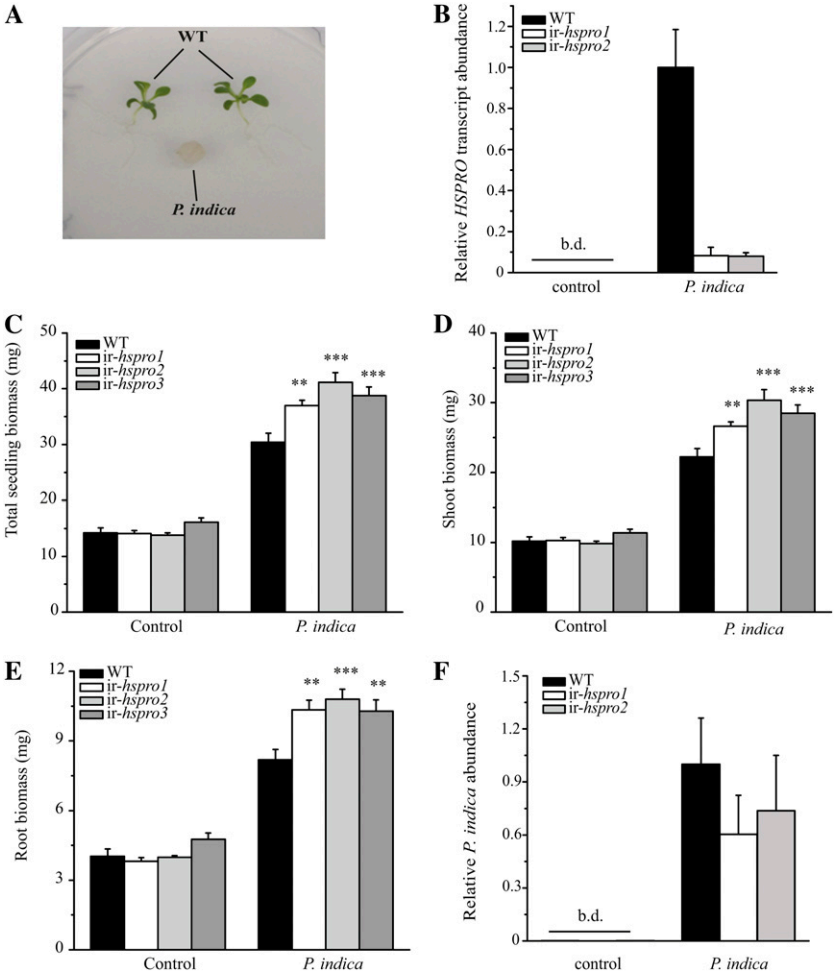

Figure 4. Induction of differential growth promotion of ir-*hspro* seedlings by *P. indica*. A, Plate system used for the experiments. Five days after germination in standard agar media, two seedlings were transferred onto a nylon mesh covering an agar plate at 1 cm distance from a plug transferred from a 2-week-old *P. indica* culture. B, Analysis of *HSPRO* mRNA levels in roots of wild-type and ir-*hspro* seedlings during interaction with *P. indica* and in control treatment (absence of *P. indica*). Root samples were harvested at day 14 ($n = 3$; bars = ±SE) and mRNA levels were quantified as detailed in caption of Figure 1. b.d., Below detection limit. C to E, Determination of the fresh biomass of total seedlings, shoots, and roots was performed with a microbalance after 14 d of seedling growth on the plate system ($n = 18$–20; bars = ±SE); one-way ANOVA with Tukey's post-hoc test (wild type versus ir-*hspro* during *P. indica* colonization); **, $P < 0.01$; ***, $P < 0.001$. F, Quantification of *P. indica* root colonization. DNA was extracted from roots of wild-type and ir-*hspro* seedlings colonized by *P. indica* at day 14 and fungal colonization was determined by qPCR based on the relative abundance of the π-*EF1a* gene compared with the Na-*EF1a* gene ($n = 16$–18; bars = ±SE). b.d., Below detection limit. [See online article for color version of this figure.]

(days 7 and 14 of the plate system) showed a close association between roots and the fungal hyphae (Supplemental Fig. S8). Similar to other plant species (Varma et al., 1999; Stein et al., 2008; Schäfer et al., 2009a; Lee et al., 2011; Zuccaro et al., 2011), the fungus colonized the maturation zone of the root without a strong association with the elongation zone and root tip (Supplemental Fig. S8). Also similar to previous observations performed with *N. attenuata* seedlings and *Sebacina vermifera* (a closely related Sebacinales species; Barazani et al., 2005), we could not detect fungal structures in the roots characteristic of endomycorrhiza (e.g. arbuscules and intracellular vesicles). Root growth and hair density after *P. indica* colonization were not different between wild-type and ir-*hspro* seedlings (Supplemental Fig. S9) and the number of secondary roots per seedling was also similar between genotypes (wild type: 5.25 ± 0.33; ir-*hspro1*: 4.50 ± 0.36; ir-*hspro2*: 4.92 ± 0.23; $n = 12$). Quantification of *P. indica* root colonization by quantitative amplification of the *P. indica EF1A* gene (Deshmukh et al., 2006) showed a lower tendency of root colonization of ir-*hspro* seedlings compared with wild-type seedlings, however the differences were not statistically significant (Fig. 4F). Hence, the differential growth promotion of ir-*hspro* seedlings was not associated with increased *P. indica* root colonization or root growth.

During colonization of Arabidopsis roots by *P. indica*, the regulation of root cell death by the fungus plays an important role (Jacobs et al., 2011; Qiang et al., 2011). When roots of *N. attenuata* wild-type and ir-*hspro* seedlings were analyzed for cell death by trypan blue staining in both the absence and presence of *P. indica* (at day 14 on the plate system), no differences in the staining pattern were observed between plant genotypes (Supplemental Fig. S10). It has been reported that the interaction of *P. indica* and closely related Sebacinales species with roots involves changes in phytohormone accumulation and signaling (Barazani et al., 2007; Stein et al., 2008; Vadassery et al., 2008; Schäfer et al., 2009b; Camehl et al., 2010). Quantification of JA, SA, abscisic acid (ABA), and ethylene (ET) levels in *P. indica*-colonized wild-type and ir-*hspro* seedlings (at day 14 on the plate system) showed that the levels of SA were reduced approximately 2-fold by root colonization but they did not differ between genotypes (Supplemental Fig. S11A). JA and ABA levels were not affected by root colonization while ET levels were induced. However, the levels of these phytohormones

were similar between genotypes (Supplemental Fig. S11B; data not shown). Interestingly, the levels of colneleic acid (CA), a divinyl-ether (DVE) derived from the action of 9-lipoxygenase (9-LOX), were strongly induced (from less than 1 nmol g fresh weight^{-1} to 40 nmol g fresh weight^{-1}) by *P. indica* in roots of both ir-*hspro* and wild-type seedlings (Supplemental Fig. S11C). These results suggested that similar to other plant species (Camehl et al., 2010; Jacobs et al., 2011; Leon-Morcillo et al., 2012), some defense-associated responses were triggered by *P. indica* in *N. attenuata* roots.

Gene Expression Profiling of ir-*hspro* Roots Reveals Significant Changes in Metabolic Processes during *P. indica* Colonization

To gain further insight into the mechanisms affected in ir-*hspro* plants, changes in gene expression in roots of ir-*hspro* and wild-type seedlings were analyzed. RNA was isolated from roots of wild-type and ir-*hspro* seedlings grown for 14 d on the plate system either in the absence or presence of *P. indica*, and changes in gene expression were evaluated with an Agilent custom array containing 43,533 *N. attenuata* probes (Gilardoni et al., 2011). This array represented approximately 70% to 80% of the *N. attenuata* transcriptome (Gase and Baldwin, 2012). Genes were considered to be differentially regulated when $\log_2$ (fold-changes [FCs]) were larger or equal to 1 or smaller or equal to −1 (ir-*hspro* versus the wild type) and *q* values were lower than 0.05 (corresponding to a false discovery rate less than 5%). Using these conditions, transcripts corresponding to 11 genes were differentially expressed in control roots of ir-*hspro* seedlings (Fig. 5A; Supplemental Table S2) while 417 genes were differentially expressed in *P. indica*-colonized roots of ir-*hspro* seedlings (Fig. 5B; Supplemental Table S2). In control roots, nine transcripts were up- and two down-regulated while in colonized roots, 293 transcripts were up-regulated and 124 were down-regulated (Fig. 5, A and B). Eight genes (all of unknown function) were differentially up-regulated in both control and *P. indica*-colonized roots (Fig. 5C; Supplemental Table S2).

In *P. indica*-colonized roots and based on the biological process, 60.6% of the annotated genes were involved in metabolic processes while 18.1% in responses to stimuli (Fig. 5D). Analysis of enzyme codes (Supplemental Tables S2 and S3), revealed that the most prevalent changes in gene expression occurred in enzymes involved in metabolic processes associated with the metabolism of starch and sugars, purines, nicotinate and nicotinamide, and membrane glycerophospholipids (Table I). Moreover, several genes involved in the transport of metabolites or ions were also affected in their expression (Table I). Gene ontology categorization by molecular function showed that genes encoding for enzymes with acyltransferase (14.2%), hydrolase (12.7%), and nucleotide binding (14.2%) activities were the most prevalent genes changing expression levels in ir-*hspro* roots (Fig. 5E; Table II). The changes in the expression of genes involved in metabolic processes were consistent with the differential growth rate of ir-*hspro* seedlings, and showed that the growth response was accompanied by significant changes in metabolic gene expression. The changes in the expression of genes involved in responses to stimuli (as the second-most prevalent group of genes; Fig. 5D) most likely reflected the processes affected in ir-*hspro* seedlings that were more directly connected with the interaction of roots with *P. indica*. The expression of several genes associated with phytohormone signaling was affected in ir-*hspro* roots and these included genes associated with JA (jasmonate zim-domain protein [JAZ], COI1), auxin (auxin response factor), and ABA (ABA INSENSITIVITY1b) signaling (Table II).

Interaction of *P. indica* with ir-*hspro* Roots Does Not Affect the Accumulation of Polar Metabolites

The changes in the expression of multiple genes involved in metabolic processes prompted us to investigate if the accumulation of primary and secondary metabolites was affected during the association of roots from ir-*hspro* seedlings with *P. indica.* For this purpose, we profiled small polar metabolites extracted from *P. indica*-colonized roots of wild-type and ir-*hspro* seedlings by liquid chromatography time-of-flight mass spectrometry. Root samples were harvested from seedlings grown for 14 d on the plate system and polar metabolites were extracted (see "Materials and Methods" for details). Ions were selected using the electrospray ionization interface in both positive and negative ion modes and those metabolites eluting from the liquid chromatography column between 125 and 550 s and having mass-to-charge ratio values ranging from 90 to 1,400 were selected for analysis. After data analysis (see "Materials and Methods" for a detailed description), no significant differences in the accumulation of ions in roots of ir-*hspro* and wild-type seedlings were detected in the negative ion mode (data not shown) and in the positive ion mode, the abundance of only three ions (out of more than 2,500 identified) changed significantly between these genotypes (Supplemental Table S4). The intensities of these ions were however low and the FCs small (between 2- and 2.8-fold down-regulated in ir-*hspro* roots).

Reduced *HSPRO* Expression in Roots Is Sufficient to Control Differential Growth Promotion in the Whole Seedling

We reasoned that if *HSPRO* had a general role associated with the control of growth instead of a more direct role in the control of the association of *P. indica* with roots, grafting experiments in which root stocks and shoot scions were reduced or not in *HSPRO* expression, could provide important information about the function of this gene. Hence, shoot scions and root stocks from either wild-type or ir-*hspro* seedlings were

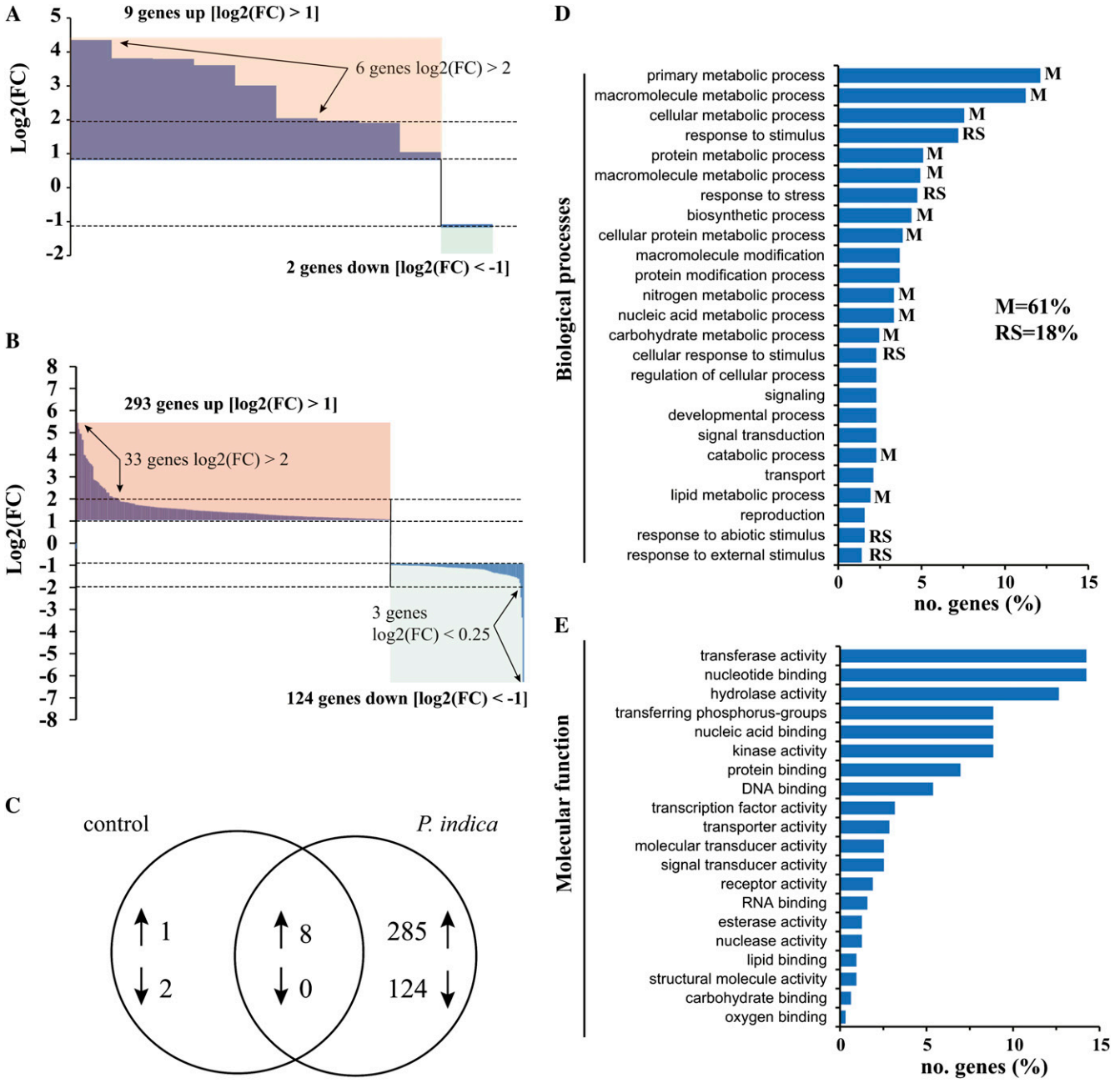

Figure 5. Microarray and Gene Ontology (GO) analysis of differentially expressed genes in *P. indica*-colonized roots of ir-*hspro* and wild-type seedlings. A, Distribution of FC of genes expressed differentially in roots of ir-*hspro* seedlings (ir-*hspro* versus the wild type). B, Distribution of FC of genes expressed differentially in roots of ir-*hspro* seedlings colonized by *P. indica* (ir-*hspro* versus the wild type). C, Venn diagram of the number of genes differentially expressed in control and colonized roots of ir-*hspro* seedlings compared with the wild type. The number in the intersection represents the genes differentially expressed in the two groups. D and E, Annotated genes differentially expressed in *P. indica*-colonized roots of ir-*hspro* seedlings were categorized based on biological processes (D) and molecular function (E), using the Blast2Go software. The numbers between brackets represent the percentage (%) of genes in the metabolism category (M) or in the stress response category (RS). [See online article for color version of this figure.]

reciprocally grafted (Fig. 6A) and the root, shoot, and seedling biomasses were quantified after 19 d of seedling growth in either the presence or absence of *P. indica*. A differential growth promotion was observed (compared with the wild type/wild-type seedlings) in all cases in which either the root stock or the shoot scion belonged to ir-*hspro* seedlings (Fig. 6, B–D). This differential growth promotion was similar to the grafted parental seedlings (ir-*hspro-1*/ir-*hspro-1* and ir-*hspro-2*/ir-*hspro-2*; Fig. 6, B–D).

Table I. *List of selected genes differentially expressed in P. indica-colonized roots of ir-hspro seedlings and involved in metabolic processes*

Gene ID	FC[a]	SD	*q* Value	Gene Description	Enzyme Codes
Starch and sugar metabolism					
Na_08858	3.4	1.1	2.8E-02	α Amylase precursor	EC:3.2.1.60; EC:3.2.1.1
Na_36852	3.0	1.0	8.7E-03	UDP-glucuronate4-epimerase3-like	EC:5.1.3.6
Na_32458	2.8	1.2	1.7E-02	Granule-bound starch synthase	EC:2.4.1.21
Na_31027	2.7	0.8	6.7E-03	β-Glucosidase41	EC:3.2.1.21
Na_36520	2.6	0.5	4.9E-03	β-Galactosidase precursor	EC:3.2.1.23
Na_16572	2.5	1.0	3.0E-02	UDP-sugar pyrophospharylase	EC:2.7.7.64
Na_33369	0.5	0.1	4.8E-03	Gal oxidase	EC:1.1.3.9
Na_42631	0.5	0.1	1.0E-02	α Glucosidase-like protein	EC:3.2.1.20
Purine metabolism					
Na_12907	3.3	1.0	1.4E-02	Nucleoside-triphosphatase	EC:3.6.1.15
Na_09592	2.8	0.2	4.0E-02	Adenosinetriphosphatase	EC:3.6.1.3
Na_26486	2.6	0.3	3.5E-02	Guanylate kinase	EC:2.7.4.8
Na_12713	2.1	0.1	1.1E-02	5′-nucleotidase	EC:3.1.3.5
Nicotinate and nicotinamide metabolism					
Na_38363	2.9	0.6	2.3E-02	Nicotinamidase	EC:3.5.1.19
Na_12713	2.1	0.2	1.1E-02	5′-nucleotidase	EC:3.1.3.5
Na_34109	2.0	0.5	2.9E-02	Aldehyde oxidase	EC:1.2.3.1
Glycerophospholipid metabolism					
Na_39990	2.1	0.3	5.7E-03	Glycerophosphodiester phosphodiesterase	EC:3.1.4.46
Na_12017	2.0	0.2	3.7E-02	Glycerol-3-phosphate dehydrogenase	EC:1.1.1.94; EC:1.1.1.8
Transport					
Na_05066	3.6	0.9	4.0E-03	Peptide transporter protein	
Na_13676	3.2	0.7	2.0E-03	Monosaccharide-sensing protein	
Na_27616	3.2	1.0	2.5E-02	Amino acid permease6	
Na_09592	2.8	0.2	4.0E-02	ATP-binding cassette transporter family protein	
Na_34386	2.3	0.3	4.9E-02	Aminophospholipid atpase	
Na_25349	2.2	0.1	1.1E-03	ATP-binding cassette transporter c family member4-like	
Na_21786	2.2	0.2	4.8E-02	Two-pore calcium channel	
Na_10110	2.1	1.1	4.9E-02	Potassium channel	
Na_27994	0.5	0.1	2.1E-03	Lipid-transfer protein	
Na_24731	0.5	0.1	7.1E-03	Bidirectional sugar transporter sweet2-like	

[a]ir-*hspro* versus the wild type.

DISCUSSION

As mentioned above, the function of $Hs1^{pro-1}$ in sugar beet was originally associated with resistance to cyst nematodes, however, several subsequent studies performed in different plant species have suggested that homologs of this gene have a more general role in the plant's response to environmental stresses (see the first section for references). Consistent with the observation that *HSPRO* homologs are induced by multiple stresses in Arabidopsis, we found that *N. attenuata HSPRO* mRNA levels were induced by multiple biotic-stress-associated stimuli including simulated lepidopteran herbivory, SA application, *Pst* DC3000 infection, and *P. indica* root colonization (Figs. 2 and 4B; Supplemental Figs. S3B and S9).

N. attenuata HSPRO Is a Negative Regulator of Seedling Growth Induced by *P. indica*

Microarray analysis of *P. indica*-colonized roots showed that silencing *HSPRO* expression brought about significant changes in gene expression and that the largest fraction (approximately 60%) of these genes were involved in metabolic processes (Fig. 5; Table I). These changes in gene expression were consistent with the accelerated growth of ir-*hspro* seedlings; increased growth rates are accompanied by increased metabolic rates to meet growth demands (e.g. cell walls and cellular membranes). Additionally, 18% of the genes affected in their expression in roots of ir-*hspro* seedlings were categorized as responses to stimuli and stresses (Fig. 5). The genes in this category probably reflected those genes having a more direct association with the interaction of roots with *P. indica* (Table II). In the absence of *P. indica* colonization, changes in gene expression in roots of ir-*hspro* plants were very small, with only 11 genes changing expression compared with wild-type seedlings (Fig. 5A). These results were consistent with a function of HSPRO in the control of metabolism during stress responses.

Similar to the interaction of roots from different plant species with arbuscular mycorrhizal fungi (Strack et al., 2003; Hause and Fester, 2005; Herrera-Medina et al., 2007), the interaction between *P. indica* and plant roots is controlled by multiple phytohomones including auxin and cytokinins (Vadassery et al., 2008), gibberellins (Schäfer et al., 2009a), ET (Barazani et al., 2007; Camehl et al., 2010), SA, and JA (Jacobs et al., 2011). Changes in

Table II. *List of selected genes differentially expressed in P. indica-colonized roots of ir-hspro seedlings and involved in regulatory processes*

Gene ID	FC[a]	SD	*q* Value	Gene Description
Transcription				
Na_10354	11.5	2.1	7.2E-05	Transcription factor Abnormal cell Lineage protein11, insulin gene enhancer protein Isl-1, Mechanosensory protein3
Na_40479	2.2	0.5	2.8E-02	No apical meristem, ATAF1 and ATAF2, CUC2 domain transcription factor
Na_31687	0.5	0.1	7.8E-03	Nuclear Protein Localization6-like
Na_26270	0.5	0.1	2.3E-02	Retinoblastoma-related protein1-like (RB1-like)
Na_06561	0.5	0.1	2.1E-02	MYB transcription factor
Na_29071	0.4	0.1	1.5E-03	MYB transcription factor
Protein kinase activity				
Na_36458	3.0	1.1	4.8E-03	Ser Thr protein kinase
Na_25553	3.0	0.6	2.3E-02	Protein kinase domain-containing protein
Na_18646	2.8	1.0	1.7E-02	Calcineurin B-Like-interacting Ser Thr-protein kinase
Na_41571	2.6	0.5	2.2E-03	Protein kinase1b
Na_18066	2.6	0.4	6.9E-03	Receptor like protein kinase-like
Na_38660	2.5	0.5	4.8E-02	Protein kinase family protein
Na_15274	2.4	0.5	1.3E-02	Tomato homolog to Arabidopsis Constitutive Triple Response2 protein
Na_26181	0.5	0.1	2.5E-02	Leu-rich repeat receptor-like protein kinase
Na_21188	0.5	0.0	4.9E-03	Leu-rich repeat protein kinase-like protein
Hormone signaling				
Na_36236	3.1	1.0	3.2E-03	Zeatin *o*-glucosyltransferase
Na_13465	2.6	1.0	4.1E-02	ABA-responsive transcription factor
Na_43242	2.5	0.6	4.1E-02	Indole-3-acetic acid-amido synthetase
Na_20394	2.3	0.7	2.2E-02	JAZ
Na_04958	2.3	0.1	2.6E-03	COI1
Na_15777	2.0	0.5	5.0E-02	Auxin response factor
Na_28242	2.0	0.5	3.0E-02	ABA INSENSITIVITY1b
Na_24453	0.5	0.0	3.6E-04	Auxin-induced saur-like protein
Na_10858	0.5	0.1	2.8E-02	ET-responsive transcription factor WIN1
Direct defense responses				
Na_00974	2.6	1.0	3.1E-02	Vicilin-like antimicrobial peptides2-1-like
Na_40698	2.0	0.4	7.2E-03	Disease resistance protein
Na_42497	0.5	0.1	6.8E-03	Callose synthase10-like

[a]ir-*hspro* versus the wild type.

the mRNA levels of auxin and ET signaling components and a cytokinin biosynthesis gene were affected in colonized roots of ir-*hspro* seedlings (Table II). Moreover, changes were also detected in the expression of COI1 and a JAZ homolog (Table II), two components of the JA-signaling pathway (Xie et al., 1998; Turner, 2007; Paschold et al., 2008). Together the results suggested that the phytohormone-signaling network was affected in ir-*hspro* plants and that these changes are probably part of the mechanisms effecting differential growth promotion of these plants during interaction with *P. indica*.

Differential expression of genes involved in ET and JA signaling in roots of wild-type and ir-*hspro* seedlings were not accompanied however by the differential accumulation of these phytohormones. The levels of JA and ABA in roots did not change during *P. indica* root colonization compared with uncolonized roots (Supplemental Fig. S11B) and although ET and SA levels were affected by *P. indica* root colonization the levels were similar between wild-type and ir-*hspro* seedlings (Supplemental Fig. S11A). The reduction in SA levels in *P. indica*-colonized roots may reflect the suppression of defense and cell death responses in *N. attenuata* seedlings. Lower SA levels in tobacco and Arabidopsis have been correlated with higher *Glomus mosseae* (Herrera Medina et al., 2003) and *P. indica* (Jacobs et al., 2011) root colonization, respectively. However, the accumulation of CA, a DVE strongly induced in leaves of Solanaceae species upon infection by *Phytophthora* spp. (Weber et al., 1999; Bonaventure et al., 2011), was also strongly induced in roots by *P. indica* in both ir-*hspro* and wild-type seedlings, indicating that oxylipin-related defense pathways were activated by this fungi (Supplemental Fig. S11C). CA is a DVE that is strongly induced in leaves of tobacco and potato (*Solanum tuberosum*) plants in response to pathogens such as *Phytophthora parasitica* and *Phytophthora infestans* (Weber et al., 1999; Göbel et al., 2002; Fammartino et al., 2007). It has been shown that DVEs have antimicrobial properties by, for example, inhibiting mycelial growth and spore germination of some

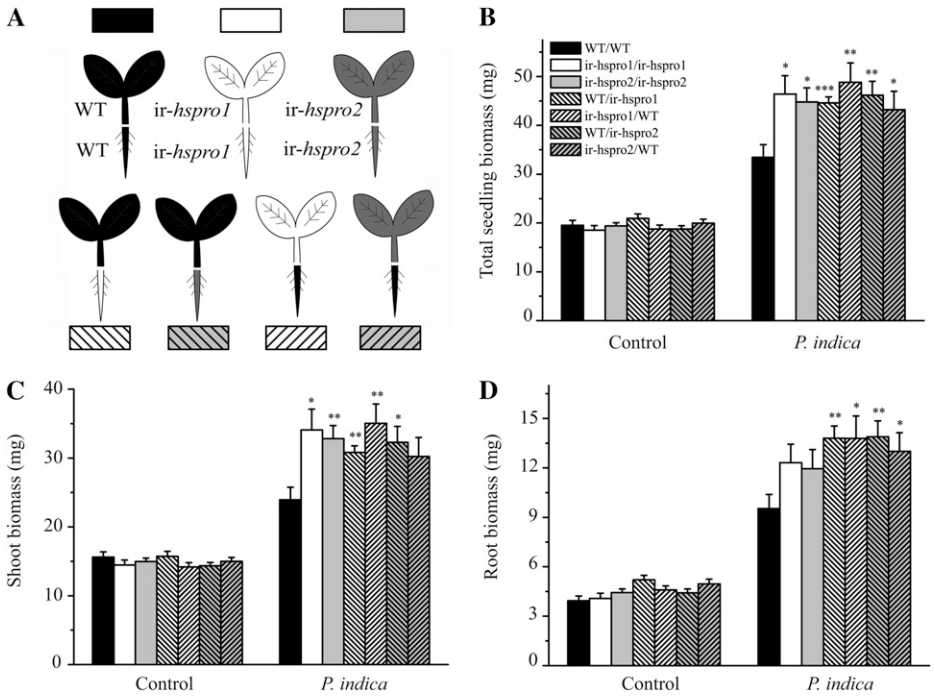

Figure 6. Reciprocal grafting of ir-*hspro* and wild-type seedlings and determination of seedling biomass during root colonization by *P. indica*. A, Scheme of the grafting combinations used. B to D, Determination of the fresh biomass of total seedlings, shoots, and roots was performed with a microbalance after 19 d of seedling growth on the plate system. One way-ANOVA with Tukey's post-hoc test (wild type versus ir-*hspro* during *P. indica* colonization); *, $P < 0.05$; **, $P < 0.01$; ***, $P < 0.001$ ($n = 18–20$; bars = ±SE).

Phytophthora species (Prost et al., 2005). Interestingly, during the interaction of *G. intraradices* with tomato (*Solanum lycopersicum*) roots, there is a strong induction of genes involved in the formation of oxylipins derived from 9-LOX activity, and it has been suggested that 9-LOX products may control arbuscular mycorrhizal fungal spread in roots (Leon-Morcillo et al., 2012).

Gene expression analysis by microarray hybridization showed only three genes directly associated with defense responses and differentially expressed in *P. indica*-colonized roots of ir-*hspro* seedlings (Supplemental Table S2). These observations were consistent with the current understanding of the mechanisms involved in the association of plant-growth-promoting rhizobacteria and fungi with roots; the activation of immune responses by plants and their suppression by microorganisms underlay the establishment of long-term mutualistic interactions (Preston, 2004; Van Wees et al., 2008; Zamioudis and Pieterse, 2012).

Grafting experiments demonstrated that the silencing of *HSPRO* expression in roots was sufficient to induce differential growth promotion in both roots and shoots of ir-*hspro* seedlings. Thus, the effect on shoot growth was dependent on the function of HSPRO in the roots. Because small-silencing RNAs generated in shoots of *N. attenuata* seedlings can be transported to roots (but not vice versa) and reduce gene expression of the targeted gene in the latter tissue (Fragoso et al., 2011), the similar effect on growth promotion observed in wild-type (shoot)/ir-*hspro* (root) and ir-*hspro* (shoot)/wild-type (root) grafted seedlings was most likely explained by shoot-induced silencing of *HSPRO* expression in roots of ir-*hspro* (shoot)/wild-type (root) grafted seedlings (Fig. 6A). Microscopy analysis of *P. indica*-colonized and uncolonized roots did not reveal morphological changes in roots of ir-*hspro* seedlings compared with the wild type, changes in the association pattern of *P. indica* with the maturation zone of the root, or differential root cell death (Supplemental Figs. S8–S10). The microbe-mediated stimulation of plant growth has been associated with improved plant nutrition via increased uptake of growth-limiting soil nutrients. Since *P. indica* root colonization and root growth was not different between ir-*hspro* and wild-type seedlings and seedlings were grown under conditions of high nutrient availability (media or soil), it is unlikely that increased uptake of growth-limiting nutrients was a main factor influencing the *P. indica*-induced differential growth promotion of ir-*hspro* seedlings. Barazani et al. (2005) showed that the nutritional status of *N. attenuata* plants colonized by *S. vermifera* and *P. indica* does not depend on N and phosphorous supply, and similar results were reported by Achatz et al. (2010) in *P. indica*-barley (*Hordeum vulgare*) symbiosis. Since growth and metabolic rates are mutually dependent, further experiments will be required to disentangle the role of *HSPRO* in the control of growth and/or metabolism. As mentioned in the introduction, the Arabidopsis HSPRO1 and HSPRO2 proteins interact with the AKIN$\beta\gamma$ subunit of the SnRK1 complex (Gissot et al., 2006). Thus, although speculative at this point, one possible scenario is that HSPRO affects *N. attenuata* seedling growth and/or metabolism via its association with SnRK1.

What's the Role of HSPRO in Responses against Insects and Pathogenic Bacteria?

Herbivore attack elicits metabolically costly defenses that can decrease plant fitness by limiting metabolic resources otherwise invested in growth and reproduction (Schwachtje and Baldwin, 2008; Bolton, 2009). The performance of *M. sexta* larvae and the *M. sexta*-OS elicited induction of the defense-associated metabolites nicotine, chlorogenic acid, and rutin were similar between ir-*hspro* and wild-type plants (Supplemental Fig. S4). Moreover, flower traits associated with the interaction of plants with insects were not affected in *M. sexta*-attacked or -unattacked ir-*hspro* plants (Supplemental Fig. S5). Thus, these results suggested that *HSPRO* was not directly involved in the regulation of induced defenses or plant-insect association traits.

Similarly, the performance of *Pst* DC3000 on leaves of ir-*hspro* plants was unaffected compared with wild-type plants. These results contrasted those made with Arabidopsis, where plants disrupted in *HSPRO2* expression supported increased *Pst* DC3000 growth in leaves (Murray et al., 2007). However, similar to *HSPRO2* expression in Arabidopsis (Murray et al., 2007), *N. attenuata HSPRO* was also induced by SA and *Pst* DC3000 infection (Fig. 2; Supplemental Fig. S3), suggesting these two genes have both overlapping and divergent functions during bacterial infection in these two plant species.

Although speculative at this point, one possible scenario is that *HSPRO* regulates plant tolerance mechanisms against insect herbivores. In *N. attenuata*, the mRNA levels of GAL83 (a β-subunit of SnRK1) are rapidly repressed upon insect herbivory and it has been shown that GAL83 is involved in the regulation of tolerance to insect herbivory via the control of resource allocation in roots (Schwachtje et al., 2006). Thus, one possibility is that the *HSPRO* gene product in *N. attenuata* participates in the regulation of tolerance mechanisms associated with the regulation of SnRK1 activity.

Plant responses to insect herbivores can also involve changes in the association of roots with belowground beneficial microorganisms such as growth-promoting fungi and rhizobacteria (Bardgett et al., 1998; Pineda et al., 2010). For example, insect herbivory can affect mycorrhizal colonization (Gehring and Whitham, 1991; Gehring and Bennett, 2009) or the composition of the root-associated microbial community (Sthultz et al., 2009). Thus, although speculative at this point, but given the results obtained with *P. indica*, an alternative (but not excluding) scenario is that *HSPRO* participates in mechanisms that control the interaction of herbivore-attacked plants with belowground microorganisms (e.g. via changes in nutrient allocation and root exudates). Plants interacting with beneficial microbes can benefit from an increase in tolerance to herbivory, for example, by affecting C and N reallocation used for tissue regrowth after herbivory (Bardgett et al., 1998). Additionally, plants can also benefit via increased resistance to plant pathogens (Pineda et al., 2010). However, association with beneficial microorganisms can also reduce plant fitness by compromising induced defense responses against insect herbivores (Barazani et al., 2005). Thus, a delicate balance of interactions between roots and microorganisms is required to optimize plant fitness in nature and *HSPRO* may play a role in this process. These hypotheses are the focus of future research.

CONCLUSION

The results presented in this study have unraveled the important role that *HSPRO* has in the control of early *N. attenuata* seedling growth stimulated by the growth-promoting fungus *P. indica*. Since the effect on growth was only observed when ir-*hspro* seedlings were colonized by this fungus, and *HSPRO* expression was induced by multiple stress-associated stimuli, the results suggested that *HSPRO* plays an important role in growth and/or metabolism readjustment during stress responses. Although speculative, the control over metabolism during insect herbivory could involve the regulation of resource partitioning between shoots and roots and its resulting consequences in the interaction of roots with soilborne microbes. The results opened new hypotheses on how this control may be achieved, and the interaction of HSPRO with components of the SnRK1 complex appears as one potential scenario. Future work will focus on the disentangling of the *HSPRO*-dependent mechanisms underlying the regulation of growth/metabolism during stress responses.

MATERIALS AND METHODS

Please refer to online Supplemental Materials and Methods S1 for additional experimental details.

Plant Growth and Treatments

Seeds of the 31st generation of an inbred genotype of *Nicotiana attenuata*, originally collected from southwestern Utah in 1988, were used for all experiments. For glasshouse experiments, seeds from wild-type and genetically transformed plants were germinated as previously described (Krügel et al., 2002). Plants were grown in the glasshouse under high-pressure sodium lamps (200–300 μmol s^{-1} m^{-2} light) with a day/night cycle of 16 h (26°C–28°C)/8 h (22°C–24°C) and 45% to 55% humidity. For plate experiments with *Piriformospora indica* see section "*P. indica* Maintenance and Inoculation of *N. attenuata* Seedlings" below. *N. attenuata* ir-*lox3* (Allmann et al., 2010), ir-*jar4/6* (Kang et al., 2006), ir-*coi1* (Paschold et al., 2008), and ir-*sipk* (Wu et al., 2007) plants have been previously described.

For wounding and elicitation treatments, leaves were wounded by rolling a fabric-pattern wheel three times on each side of the midvein and the wounds were supplemented either with 10 μL of 0.01% (v/v) Tween 20 in water (wounding treatment), 10 μL of 18:3-Glu (0.03 nmol/μL; FAC elicitation), or 10 μL of *Manduca sexta* or *Spodoptera exigua* OS (OS elicitation). For analysis of gene expression, *Pseudomonas syringae* pv *tomato* (*Pst*) DC3000 and *Agrobacterium tumefaciens* (GV3101) were grown on Luria-Bertani liquid medium containing 25 μg mL^{-1} Rifampicin until optical density at 600 nm (OD_{600}) = 0.5 to 0.6. Bacteria were pelleted and resuspended in 10 mM $MgCl_2$ to a final OD_{600} = 0.02 (10^7 CFU mL^{-1}). This suspension was syringe infiltrated into leaves (1 mL $leaf^{-1}$). As control treatment, leaves were infiltrated with an aqueous solution of 10 mM $MgCl_2$. For infection assays with *Pst* DC3000, the bacteria pellet was resuspended in 10 mM $MgCl_2$ to a final OD_{600} = 0.001 (10^5 CFU mL^{-1}) and the

suspension was syringe infiltrated into leaves (1 mL leaf^{-1}). Leaf discs of 8 mm in diameter were harvested at different times (0, 1, 2, and 3 d), ground in 0.3 mL of sterile water, and after centrifugation, one-tenth serial dilutions of the supernatant were plated out on Luria-Bertani agar plates containing 25 μg mL^{-1} Rifampicin. Plates were incubated for 2 d at 28°C and the CFU were counted. For SA treatment, a solution of 300 μM SA dissolved in 0.2% (v/v) Tween 20/water was used. The solvent alone was used as control treatment. Tissue expression profile of *HSPRO* was evaluated by collecting different plant tissues from wild-type *N. attenuata* plants; rosette leaves and roots were collected from 30-d-old (rosette stage) plants whereas stalks, stalk leaves, sepals, pistils, corolla, and stamens were collected from 50-d-old plants.

Generation of Stably Silenced Lines

A PCR fragment generated with primers ir-hspro-fwd and ir-hspro-rev (Supplemental Table S5) and *HSPRO* complementary DNA as template was subcloned using *Sac*I and *Xho*I (New England Biolabs) restriction sites into the pSOL8 transformation vector (Bubner et al., 2006) as an inverted-repeat construct. This construct was used to transform *N. attenuata* wild-type plants using *A. tumefaciens*-mediated transformation and plant regeneration as previously described (Krügel et al., 2002). T1 transformed plants were analyzed for T-DNA insertion number by DNA gel-blot hybridization (see below). Segregation analysis for hygromycin resistance in T2 seedlings was performed on agar plates supplemented with hygromycin (0.035 mg mL^{-1}). Two lines, ir-*hspro*1 and ir-*hspro*2 had a single T-DNA insertion in their genomes, and were used for most of the experiments. A third line, ir-*hspro*3 had two T-DNA insertions and was used for some experiments. Efficiency of gene silencing (*HSPRO* mRNA levels) in ir-*hspro* plants was evaluated by quantitative real-time PCR (qPCR; see below) after 1 h of 18:3-Glu elicitation using the primers listed in Supplemental Table S5. For Southern-blot analysis, genomic DNA from wild-type and ir-*hspro* plants was isolated by the cetyltrimethylammonium bromide method. DNA samples (5 μg) were digested with *Eco*RV (New England Biolabs) overnight at 37°C according to commercial instructions and separated on a 0.8% (w/v) agarose gel using standard conditions. DNA was blotted onto gene screen plus hybridization transfer membranes (Perkin Elmer Life and Analytical Sciences) using the capillary transfer method. A gene-specific probe for the hygromycin resistance gene *hptII* was generated by PCR using the primers HYG1-18 and HYG3-20 (Supplemental Table S5). The probe was labeled with [α-^{32}P]dCTP (Perkin Elmer) using the Rediprime II kit (Amersham Pharmacia) according to commercial instructions.

P. indica Maintenance and Colonization of *N. attenuata* Seedlings

P. indica was maintained on Kaefer medium (a modified *Aspergillus* spp. minimal medium; Pham et al., 2004) containing 1% (w/v) agar. For seedling colonization, 9-cm discs of polyamide mesh (pore 70 μm/thickness 80 μm; SEFAR GmbH) were placed on top of 9-cm agar plates containing modified plant nutrient culture medium [5 mM KNO_3, 2 mM $MgSO_4$, 2 mM $Ca(NO_3)_2$, 0.01 μM $FeSO_4$, 70 μM H_3BO_3, 14 μM $MnCl_2$, 0.5 μM $CuSO_4$, 1 μM $ZnSO_4$, 0.2 μM Na_2MoO_4, 0.01 μM $CoCl_2$, 10.5 g L^{-1} agar, pH 5.6, 0.6% (w/v) agar]. Two 7-d-old *N. attenuata* seedlings germinated on Gamborg's B5 medium (pH: 6.8; 0.6% [w/v] agar) were laid on the polyamide discs at a distance of 1 cm from an agar plug placed in the center of the plate and containing a 2-week-old *P. indica* culture (Fig. 4A). Agar plugs without fungus were used as control. The plates were incubated horizontally for 10 or 14 d at 21°C and light was supplied from the side for 16 h d^{-1} with a white fluorescent light source (80 μmol m^{-2} s^{-1}). The fresh biomass of total seedlings, roots, and shoots was determined with a microbalance. Seedling grafting was performed as previously described (Fragoso et al., 2011). After grafting, seedlings were first kept for 5 d on Gamborg's B5 medium containing 0.8% (w/v) agar for recovery and were then transferred to agar plates covered with polyamide mesh discs and preincubated (7 d before) with *P. indica* agar plugs. The fresh biomass of total seedlings, roots, and shoots was determined in this case 19 d after the transferring of the seedlings to the *P. indica*-containing plates (due to the slower growth of grafted seedlings compared with intact seedlings).

qPCR

Total RNA was extracted using the TRIzol reagent (Invitrogen) and 5 μg of total RNA were reverse transcribed using oligo(dT)$_{18}$ and SuperScript reverse transcriptase II (Invitrogen). qPCR was performed with a Mx3005P Multiplex qPCR system (Stratagene) and the qPCR core kit for SYBR Green I (Eurogentec). Relative quantification of *HSPRO* mRNA levels was performed by the comparative cycle threshold method using the elongation factor 1A (Na-*EF1A*) mRNA as an internal standard (Gilardoni et al., 2010). The sequences of the primers used for qPCR are listed in Supplemental Table S5. All the reactions were performed using the following qPCR conditions: initial denaturation step of 95°C for 10 min, followed by 40 cycles each of 95°C for 15 s and 60°C for 1 min, with a final extension step of 95°C for 15 s and 60°C for 30 s. All samples were obtained from at least three independent biological replicates (n = 3) for each time point, plant genotype, and treatment.

For quantification of *P. indica* colonization rates, DNA was extracted from *P. indica*-colonized roots and control roots by the cetyltrimethylammonium bromide method. qPCR was performed using SYBR Green and 20 ng of isolated DNA as template. Copy number of the *P. indica* translation elongation factor 1a (π-*EF1A*) gene (Deshmukh et al., 2006) relative to the Na-*EF1A* gene was used to quantify colonization rates of *P. indica* by the comparative cycle threshold method. The primers used are listed in Supplemental Table S5.

Statistical Analysis

Statistics were calculated using the SPSS software version 17.0. The data were subjected to one-way ANOVA (and means were compared by the Tukey's post-hoc test). For analysis of differences in bolting and flowering time the Kolmogorov-Smirnov test was used. The number of replicates (n) used in each experiment are detailed in the figures' captions.

Data from this article can be found under the following accession numbers: Na-HSPRO (JQ354963; GenBank database), Agilent Chip platform (GPL13527; National Center for Biotechnology Information Gene Expression Omnibus database), microarray data (GSE35086; National Center for Biotechnology Information Gene Expression Omnibus database).

Supplemental Data

The following materials are available in the online version of this article.

Supplemental Figure S1. Alignment of *N. attenuata* HSPRO protein sequence with close homologs in different plant and moss species.

Supplemental Figure S2. Alignment of *N. attenuata* HSPRO protein sequence with homologs in Arabidopsis and *B. procumbens*.

Supplemental Figure S3. Analysis of *HSPRO* expression in wild-type plants and in transgenic plants reduced in MAP kinase expression.

Supplemental Figure S4. Analysis of defense responses against *M. sexta* in wild-type and ir-*hspro* plants.

Supplemental Figure S5. Analysis of flower traits associated with the interactions of *N. attenuata* plants with insects.

Supplemental Figure S6. Analysis of growth and developmental parameters of *P. indica*-colonized plants grown in the glasshouse.

Supplemental Figure S7. Analysis of growth promotion of wild-type and ir-*hspro* seedlings induced by *P. indica* in a split-plate system.

Supplemental Figure S8. Laser confocal microscopy analysis of roots from *P. indica*-colonized wild-type and ir-*hspro* seedlings.

Supplemental Figure S9. Root morphology of *P. indica*-colonized wild-type and ir-*hspro* seedlings.

Supplemental Figure S10. Analysis of root cell death in wild-type and ir-*hspro* seedlings.

Supplemental Figure S11. Analysis of SA, JA, and CA levels in roots of wild-type and ir-*hspro* seedlings.

Supplemental Table S1. Analysis of wild-type and ir-*hspro* seedling's biomasses during *P. indica*-root colonization and control treatments.

Supplemental Table S2. List of genes changing expression in control and *P. indica*-colonized roots of ir-*hspro* seedlings compared with the wild type.

Supplemental Table S3. List of annotated genes involved in metabolism and with enzyme codes differentially expressed in *P.indica*-colonized roots of ir-*hspro* seedlings.

Supplemental Table S4. List of ions with differential accumulation in *P. indica*-colonized roots of ir-*hspro* seedlings compared with wild-type seedlings (positive mode of ionization).

Supplemental Table S5. List of primers.

Supplemental Materials and Methods S1.

ACKNOWLEDGMENTS

The authors would like to thank Dr. J. Wu for supplying Gateway cloning material and for his assistance during cloning and protoplast transfection, V. Fragoso for her help with seedling grafting, and A. Wissgott for her help with microarrays.

Received July 20, 2012; accepted August 14, 2012; published August 14, 2012.

LITERATURE CITED

Achatz B, Kogel KH, Franken P, Waller F (2010) Piriformospora indica mycorrhization increases grain yield by accelerating early development of barley plants. Plant Signal Behav **5:** 1685–1687

Allmann S, Halitschke R, Schuurink RC, Baldwin IT (2010) Oxylipin channelling in *Nicotiana attenuata*: lipoxygenase 2 supplies substrates for green leaf volatile production. Plant Cell Environ **33:** 2028–2040

Baena-González E, Sheen J (2008) Convergent energy and stress signaling. Trends Plant Sci **13:** 474–482

Baldwin IT, Morse L (1994) Up in smoke 2: germination of Nicotiana attenuata in response to smoke-derived cues and nutrients in burned and unburned soils. J Chem Ecol **20:** 2373–2391

Baldwin IT, Preston CA (1999) The eco-physiological complexity of plant responses to insect herbivores. Planta **208:** 137–145

Barazani O, Benderoth M, Groten K, Kuhlemeier C, Baldwin IT (2005) Piriformospora indica and Sebacina vermifera increase growth performance at the expense of herbivore resistance in Nicotiana attenuata. Oecologia **146:** 234–243

Barazani O, von Dahl CC, Baldwin IT (2007) *Sebacina vermifera* promotes the growth and fitness of *Nicotiana attenuata* by inhibiting ethylene signaling. Plant Physiol **144:** 1223–1232

Bardgett RD, Wardle DA, Yeates GW (1998) Linking above-ground and below-ground interactions: how plant responses to foliar herbivory influence soil organisms. Soil Biol Biochem **30:** 1867–1878

Bolton MD (2009) Primary metabolism and plant defense—fuel for the fire. Mol Plant Microbe Interact **22:** 487–497

Bonaventure G, Schuck S, Baldwin IT (2011) Revealing complexity and specificity in the activation of lipase-mediated oxylipin biosynthesis: a specific role of the Nicotiana attenuata GLA1 lipase in the activation of jasmonic acid biosynthesis in leaves and roots. Plant Cell Environ **34:** 1507–1520

Bubner B, Gase K, Berger B, Link D, Baldwin IT (2006) Occurrence of tetraploidy in Nicotiana attenuata plants after Agrobacterium-mediated transformation is genotype specific but independent of polysomaty of explant tissue. Plant Cell Rep **25:** 668–675

Cai D, Kleine M, Kifle S, Harloff HJ, Sandal NN, Marcker KA, Klein-Lankhorst RM, Salentijn EMJ, Lange W, Stiekema WJ, et al (1997) Positional cloning of a gene for nematode resistance in sugar beet. Science **275:** 832–834

Camehl I, Drzewiecki C, Vadassery J, Shahollari B, Sherameti I, Forzani C, Munnik T, Hirt H, Oelmüller R (2011) The OXI1 kinase pathway mediates Piriformospora indica-induced growth promotion in Arabidopsis. PLoS Pathog **7:** e1002051

Camehl I, Sherameti I, Venus Y, Bethke G, Varma A, Lee J, Oelmüller R (2010) Ethylene signalling and ethylene-targeted transcription factors are required to balance beneficial and nonbeneficial traits in the symbiosis between the endophytic fungus Piriformospora indica and Arabidopsis thaliana. New Phytol **185:** 1062–1073

Cominelli E, Galbiati M, Vavasseur A, Conti L, Sala T, Vuylsteke M, Leonhardt N, Dellaporta SL, Tonelli C (2005) A guard-cell-specific MYB transcription factor regulates stomatal movements and plant drought tolerance. Curr Biol **15:** 1196–1200

Deshmukh S, Hückelhoven R, Schäfer P, Imani J, Sharma M, Weiss M, Waller F, Kogel KH (2006) The root endophytic fungus Piriformospora indica requires host cell death for proliferation during mutualistic symbiosis with barley. Proc Natl Acad Sci USA **103:** 18450–18457

Fakhro A, Andrade-Linares DR, von Bargen S, Bandte M, Büttner C, Grosch R, Schwarz D, Franken P (2010) Impact of Piriformospora indica on tomato growth and on interaction with fungal and viral pathogens. Mycorrhiza **20:** 191–200

Fammartino A, Cardinale F, Göbel C, Mène-Saffrané L, Fournier J, Feussner I, Esquerré-Tugayé MT (2007) Characterization of a divinyl ether biosynthetic pathway specifically associated with pathogenesis in tobacco. Plant Physiol **143:** 378–388

Fragoso V, Goddard H, Baldwin IT, Kim SG (2011) A simple and efficient micrografting method for stably transformed Nicotiana attenuata plants to examine shoot-root signaling. Plant Methods **7:** 34

Fujita M, Mizukado S, Fujita Y, Ichikawa T, Nakazawa M, Seki M, Matsui M, Yamaguchi-Shinozaki K, Shinozaki K (2007) Identification of stress-tolerance-related transcription-factor genes via mini-scale full-length cDNA Over-eXpressor (FOX) gene hunting system. Biochem Biophys Res Commun **364:** 250–257

Gase K, Baldwin IT (2012) Transformational tools for next generation ecology: manipulation of gene expression remains the gold standard for the functional analyses of genes. Plant Ecol Divers (in press)

Gehring C, Bennett A (2009) Mycorrhizal fungal-plant-insect interactions: the importance of a community approach. Environ Entomol **38:** 93–102

Gehring CA, Whitham TG (1991) Herbivore-driven mycorrhizal mutualism in insect-susceptible pinyon pine. Nature **353:** 556–557

Gilardoni PA, Hettenhausen C, Baldwin IT, Bonaventure G (2011) *Nicotiana attenuata* LECTIN RECEPTOR KINASE1 suppresses the insect-mediated inhibition of induced defense responses during *Manduca sexta* herbivory. Plant Cell **23:** 3512–3532

Gilardoni PA, Schuck S, Jüngling R, Rotter B, Baldwin IT, Bonaventure G (2010) SuperSAGE analysis of the Nicotiana attenuata transcriptome after fatty acid-amino acid elicitation (FAC): identification of early mediators of insect responses. BMC Plant Biol **10:** 66

Gissot L, Polge C, Jossier M, Girin T, Bouly JP, Kreis M, Thomas M (2006) AKINbetagamma contributes to SnRK1 heterotrimeric complexes and interacts with two proteins implicated in plant pathogen resistance through its KIS/GBD sequence. Plant Physiol **142:** 931–944

Göbel C, Feussner I, Hamberg M, Rosahl S (2002) Oxylipin profiling in pathogen-infected potato leaves. Biochim Biophys Acta **1584:** 55–64

Halford NG, Hey S, Jhurreea D, Laurie S, McKibbin RS, Paul M, Zhang Y (2003) Metabolic signalling and carbon partitioning: role of Snf1-related (SnRK1) protein kinase. J Exp Bot **54:** 467–475

Hammond JP, Bennett MJ, Bowen HC, Broadley MR, Eastwood DC, May ST, Rahn C, Swarup R, Woolaway KE, White PJ (2003) Changes in gene expression in Arabidopsis shoots during phosphate starvation and the potential for developing smart plants. Plant Physiol **132:** 578–596

Hause B, Fester T (2005) Molecular and cell biology of arbuscular mycorrhizal symbiosis. Planta **221:** 184–196

Herrera Medina M, Gagnon H, Piché Y, Ocampo JA, Garcia Garrido JM, Vierheilig H (2003) Root colonization by arbuscular mycorrhizal fungi is affected by the salicylic acid content of the plant. Plant Sci **164:** 993–998

Herrera-Medina MJ, Steinkellner S, Vierheilig H, Ocampo Bote JA, García Garrido JM (2007) Abscisic acid determines arbuscule development and functionality in the tomato arbuscular mycorrhiza. New Phytol **175:** 554–564

Jacobs S, Zechmann B, Molitor A, Trujillo M, Petutschnig E, Lipka V, Kogel KH, Schäfer P (2011) Broad-spectrum suppression of innate immunity is required for colonization of Arabidopsis roots by the fungus *Piriformospora indica*. Plant Physiol **156:** 726–740

Kallenbach M, Alagna F, Baldwin IT, Bonaventure G (2010) *Nicotiana attenuata* SIPK, WIPK, NPR1, and fatty acid-amino acid conjugates participate in the induction of jasmonic acid biosynthesis by affecting early enzymatic steps in the pathway. Plant Physiol **152:** 96–106

Kang JH, Wang L, Giri A, Baldwin IT (2006) Silencing threonine deaminase and JAR4 in *Nicotiana attenuata* impairs jasmonic acid-isoleucine-mediated defenses against *Manduca sexta*. Plant Cell **18:** 3303–3320

Krügel T, Lim M, Gase K, Halitschke R, Baldwin IT (2002) Agrobacterium-mediated transformation of Nicotiana attenuata, a model ecological expression system. Chemoecology **12:** 177–183

Kudla U, Milac AL, Qin L, Overmars H, Roze E, Holterman M, Petrescu AJ, Goverse A, Bakker J, Helder J, et al (2007) Structural and functional characterization of a novel, host penetration-related pectate lyase from

the potato cyst nematode Globodera rostochiensis. Mol Plant Pathol **8:** 293–305

Lee YC, Johnson JM, Chien CT, Sun C, Cai D, Lou B, Oelmüller R, Yeh KW (2011) Growth promotion of Chinese cabbage and Arabidopsis by Piriformospora indica is not stimulated by mycelium-synthesized auxin. Mol Plant Microbe Interact **24:** 421–431

Leon-Morcillo RJ, Angel J, Martin R, Vierheilig H, Ocampo JA, Garcia-Garrido JM (2012) Late activation of the 9-oxylipin pathway during arbuscular mycorrhiza formation in tomato and its regulation by jasmonate signalling. J Exp Bot **63:** 3545–3558

Long HH, Sonntag DG, Schmidt DD, Baldwin IT (2010) The structure of the culturable root bacterial endophyte community of Nicotiana attenuata is organized by soil composition and host plant ethylene production and perception. New Phytol **185:** 554–567

Lovas A, Bimbó A, Szabó L, Bánfalvi Z (2003) Antisense repression of StubGAL83 affects root and tuber development in potato. Plant J **33:** 139–147

Luhua S, Ciftci-Yilmaz S, Harper J, Cushman J, Mittler R (2008) Enhanced tolerance to oxidative stress in transgenic Arabidopsis plants expressing proteins of unknown function. Plant Physiol **148:** 280–292

Murray SL, Ingle RA, Petersen LN, Denby KJ (2007) Basal resistance against Pseudomonas syringae in Arabidopsis involves WRKY53 and a protein with homology to a nematode resistance protein. Mol Plant Microbe Interact **20:** 1431–1438

Paschold A, Bonaventure G, Kant MR, Baldwin IT (2008) Jasmonate perception regulates jasmonate biosynthesis and JA-Ile metabolism: the case of COI1 in Nicotiana attenuata. Plant Cell Physiol **49:** 1165–1175

Pham GH, Kumari R, Singh A, Sachdev M, Prasad R, Kaldorf M, Buscot F, Oelmüller R, Peskan T, Weiss M, Hampp R, et al (2004) Axenic cultures of *Piriformospora indica. In* Plant Surface Microbiology. Springer, Berlin, pp 593–616

Pineda A, Zheng SJ, van Loon JJ, Pieterse CM, Dicke M (2010) Helping plants to deal with insects: the role of beneficial soil-borne microbes. Trends Plant Sci **15:** 507–514

Preston GM (2004) Plant perceptions of plant growth-promoting Pseudomonas. Philos Trans R Soc Lond B Biol Sci **359:** 907–918

Prost I, Dhondt S, Rothe G, Vicente J, Rodriguez MJ, Kift N, Carbonne F, Griffiths G, Esquerré-Tugayé MT, Rosahl S, et al (2005) Evaluation of the antimicrobial activities of plant oxylipins supports their involvement in defense against pathogens. Plant Physiol **139:** 1902–1913

Puthoff DP, Nettleton D, Rodermel SR, Baum TJ (2003) Arabidopsis gene expression changes during cyst nematode parasitism revealed by statistical analyses of microarray expression profiles. Plant J **33:** 911–921

Qiang X, Weiss M, Kogel KH, Schafer P (2011) Piriformospora indica—a mutualistic basidiomycete with an exceptionally large plant host range. Mol Plant Pathol **13:** 508–518

Rosenthal JP, Kotanen PM (1994) Terrestrial plant tolerance to herbivory. Trends Ecol Evol **9:** 145–148

Sahay NS, Varma A (1999) Piriformospora indica: a new biological hardening tool for micropropagated plants. FEMS Microbiol Lett **181:** 297–302

Schäfer P, Pfiffi S, Voll LM, Zajic D, Chandler PM, Waller F, Scholz U, Pons-Kühnemann J, Sonnewald S, Sonnewald U, et al (2009a) Manipulation of plant innate immunity and gibberellin as factor of compatibility in the mutualistic association of barley roots with Piriformospora indica. Plant J **59:** 461–474

Schäfer P, Pfiffi S, Voll LM, Zajic D, Chandler PM, Waller F, Scholz U, Pons-Kühnemann J, Sonnewald S, Sonnewald U, et al (2009b) Phytohormones in plant root-Piriformospora indica mutualism. Plant Signal Behav **4:** 669–671

Schwachtje J, Baldwin IT (2008) Why does herbivore attack reconfigure primary metabolism? Plant Physiol **146:** 845–851

Schwachtje J, Minchin PEH, Jahnke S, van Dongen JT, Schittko U, Baldwin IT (2006) SNF1-related kinases allow plants to tolerate herbivory by allocating carbon to roots. Proc Natl Acad Sci USA **103:** 12935–12940

Stein E, Molitor A, Kogel KH, Waller F (2008) Systemic resistance in Arabidopsis conferred by the mycorrhizal fungus Piriformospora indica requires jasmonic acid signaling and the cytoplasmic function of NPR1. Plant Cell Physiol **49:** 1747–1751

Sthultz CM, Whitham TG, Kennedy K, Deckert R, Gehring CA (2009) Genetically based susceptibility to herbivory influences the ectomycorrhizal fungal communities of a foundation tree species. New Phytol **184:** 657–667

Strack D, Fester T, Hause B, Schliemann W, Walter MH (2003) Arbuscular mycorrhiza: biological, chemical, and molecular aspects. J Chem Ecol **29:** 1955–1979

Turner JG (2007) Stress responses: JAZ players deliver fusion and rhythm. Curr Biol **17:** R847–R849

Vadassery J, Ritter C, Venus Y, Camehl I, Varma A, Shahollari B, Novák O, Strnad M, Ludwig-Müller J, Oelmüller R (2008) The role of auxins and cytokinins in the mutualistic interaction between Arabidopsis and Piriformospora indica. Mol Plant Microbe Interact **21:** 1371–1383

Van Wees SCM, Van der Ent S, Pieterse CMJ (2008) Plant immune responses triggered by beneficial microbes. Curr Opin Plant Biol **11:** 443–448

Varma A, Savita Verma, Sudha , Sahay N, Butehorn B, Franken P (1999) Piriformospora indica, a cultivable plant-growth-promoting root endophyte. Appl Environ Microbiol **65:** 2741–2744

Waller F, Achatz B, Baltruschat H, Fodor J, Becker K, Fischer M, Heier T, Hückelhoven R, Neumann C, von Wettstein D, et al (2005) The endophytic fungus Piriformospora indica reprograms barley to salt-stress tolerance, disease resistance, and higher yield. Proc Natl Acad Sci USA **102:** 13386–13391

Walley JW, Coughlan S, Hudson ME, Covington MF, Kaspi R, Banu G, Harmer SL, Dehesh K (2007) Mechanical stress induces biotic and abiotic stress responses via a novel cis-element. PLoS Genet **3:** 1800–1812

Weber H, Chételat A, Caldelari D, Farmer EE (1999) Divinyl ether fatty acid synthesis in late blight-diseased potato leaves. Plant Cell **11:** 485–494

Weiss M, Selosse MA, Rexer KH, Urban A, Oberwinkler F (2004) Sebacinales: a hitherto overlooked cosm of heterobasidiomycetes with a broad mycorrhizal potential. Mycol Res **108:** 1003–1010

Wu JQ, Hettenhausen C, Meldau S, Baldwin IT (2007) Herbivory rapidly activates MAPK signaling in attacked and unattacked leaf regions but not between leaves of *Nicotiana attenuata*. Plant Cell **19:** 1096–1122

Xie DX, Feys BF, James S, Nieto-Rostro M, Turner JG (1998) COI1: an Arabidopsis gene required for jasmonate-regulated defense and fertility. Science **280:** 1091–1094

Zamioudis C, Pieterse CM (2012) Modulation of host immunity by beneficial microbes. Mol Plant Microbe Interact **25:** 139–150

Zipfel C, Robatzek S, Navarro L, Oakeley EJ, Jones JD, Felix G, Boller T (2004) Bacterial disease resistance in Arabidopsis through flagellin perception. Nature **428:** 764–767

Zuccaro A, Lahrmann U, Güldener U, Langen G, Pfiffi S, Biedenkopf D, Wong P, Samans B, Grimm C, Basiewicz M, et al (2011) Endophytic life strategies decoded by genome and transcriptome analyses of the mutualistic root symbiont Piriformospora indica. PLoS Pathog **7:** e1002290

A

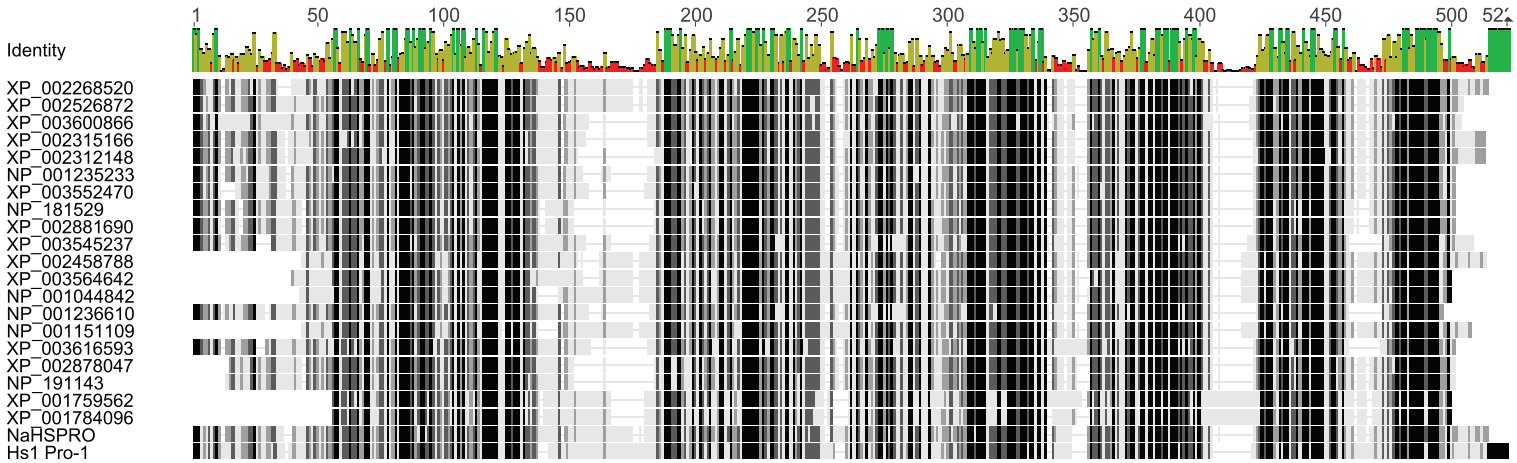

B

GenBank annotation	E-Value (blastx)	Gene ID	Organism	% Pairwise Identity
Nicotiana attenuata HSPRO	**0**	**NaHSPRO** (JQ354963)	***Nicotiana attenuata***	**100**
nematode resistance protein-like HSPRO2 isoform 1	0	XP_002268520	*Vitis vinifera*	69
conserved hypothetical protein	0	XP_002526872	*Ricinus communis*	68
predicted protein	0	XP_002315166	*Populus trichocarpa* (2)	64
Beta procumbens nematode resistance (Hs1pro-1)	0	combined AAB48305 and AAZ39087	*Beta procumbes*	63
predicted protein	0	XP_002312148	*Populus trichocarpa* (1)	61
uncharacterized protein LOC547603	0	NP_001235233	*Glycine max* (1)	58
PREDICTED: nematode resistance protein-like HSPRO2-like	0	XP_003552470	*Glycine max* (2)	58
hypothetical protein MTR_3g070230	0	XP_003600866	*Medicago truncatula*	58
PREDICTED: nematode resistance protein-like HSPRO1-like	4.14E-166	XP_003564642	*Brachypodium distachyon*	53
HS1 PRO-1 2-like protein (HSPRO2)	2.62E-175	NP_181529 (At3g55840)	*Arabidopsis thaliana* (1)	53
nematode-resistance protein	4.83E-163	NP_001151109	*Zea mays*	53
hypothetical protein ARALYDRAFT_483040	9.82E-170	XP_002881690	*Arabidopsis lyrata* (1)	53
Os01g0855600	1.01E-163	NP_001044842	*Oryza sativa*	53
hypothetical protein SORBIDRAFT_03g040300	3.51E-166	XP_002458788	*Sorghum bicolor*	53
nematode resistance HS1pro1 protein	3.66E-163	NP_001236610	*Glycine max* (4)	51
hypothetical protein ARALYDRAFT_486026	2.49E-155	XP_002878047	*Arabidopsis lyrata* (2)	51
Hs1pro-1 protein (HSPRO1)	1.69E-154	NP_191143 (At2g4000)	*Arabidopsis thaliana* (2)	50
PREDICTED: nematode resistance protein-like HSPRO2-like	7.50E-168	XP_003545237	*Glycine max* (3)	50
Nematode resistance HS1pro1 protein	1.31E-157	XP_003616593	*Medicago truncatula*	48
predicted protein	1.40E-124	XP_001759562	*Physcomitrella patens* (1)	45
predicted protein	1.28E-122	XP_001784096	*Physcomitrella patens* (2)	45

Supplemental Figure S1. Alignment of *N. attenuata* HSPRO protein sequence with close homologs in different plant species.

(a) Schematic protein sequence alignment of *N. attenuata* HSPRO (JQ354963) with the 21 closest homologs in different plant species deposited in GenBank (including *B. procumbens* $Hs1^{pro\text{-}1}$). The cartoon above the sequences shows the % of similarity (green bars within the overlapping regions represent identical amino acids). See materials and methods for alignment parameters. **(b)** Reference table for genes, accesion numbers and species used in (a) and Figure 1b.c

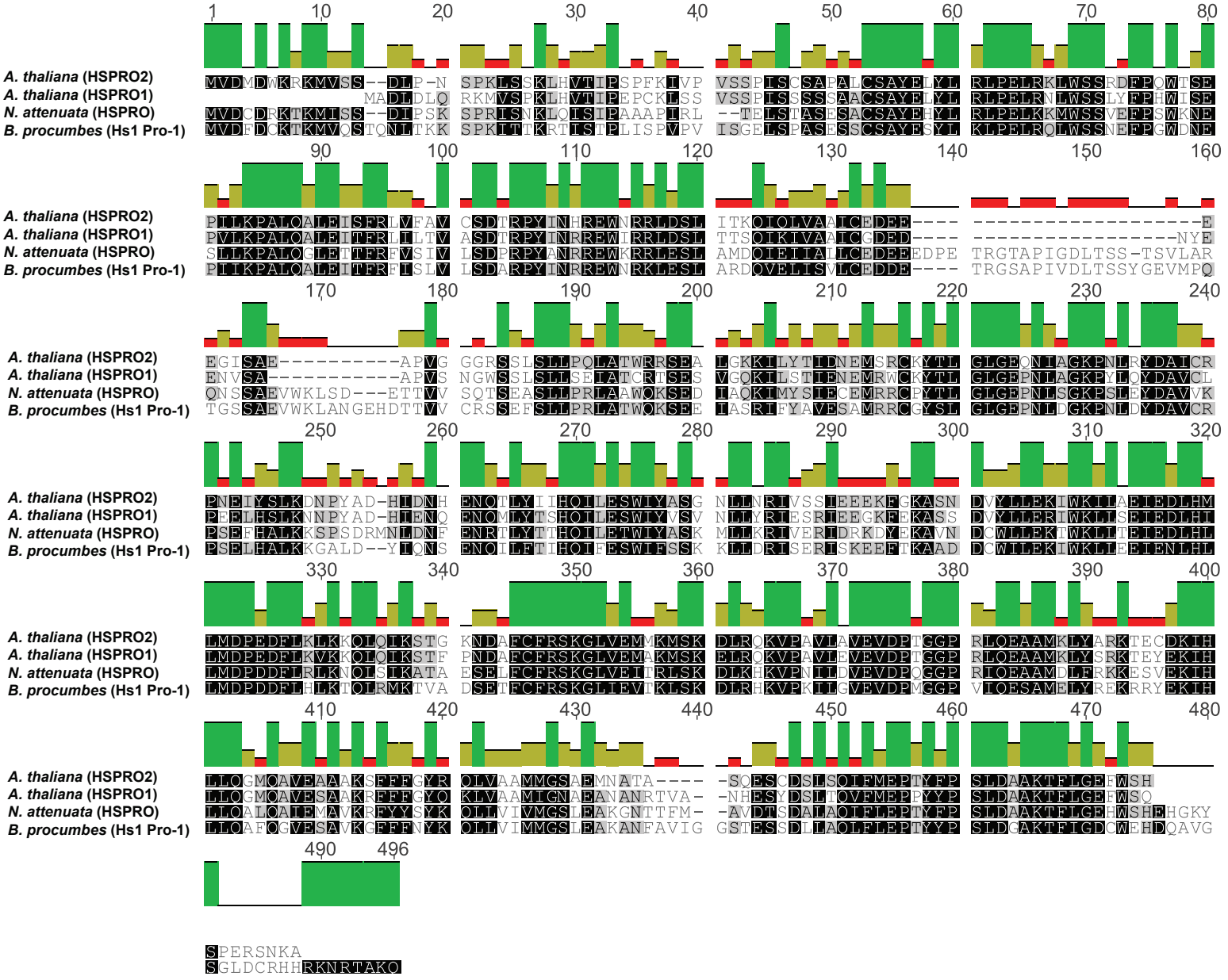

Supplemental Figure S2. Alignment of *N. attenuata* HSPRO protein sequence with homologs in *A. thaliana* and *B. procumbens*.

N. attenuata HSPRO (JQ354963); Arabidopsis HSPRO1 (NP_191143; At2g4000), Arabidopsis HSPRO2 (NP_181529; At3g55840), full lenght sugar beet (*B. procumbes)* Hs1^{pro-1} (combined AAB48305 and AAZ39087). The cartoon above the sequences represent the % of similarity (green bars within the overlapping regions shows identical amino acids in the four sequences). See materials and methods for alignment parameters.

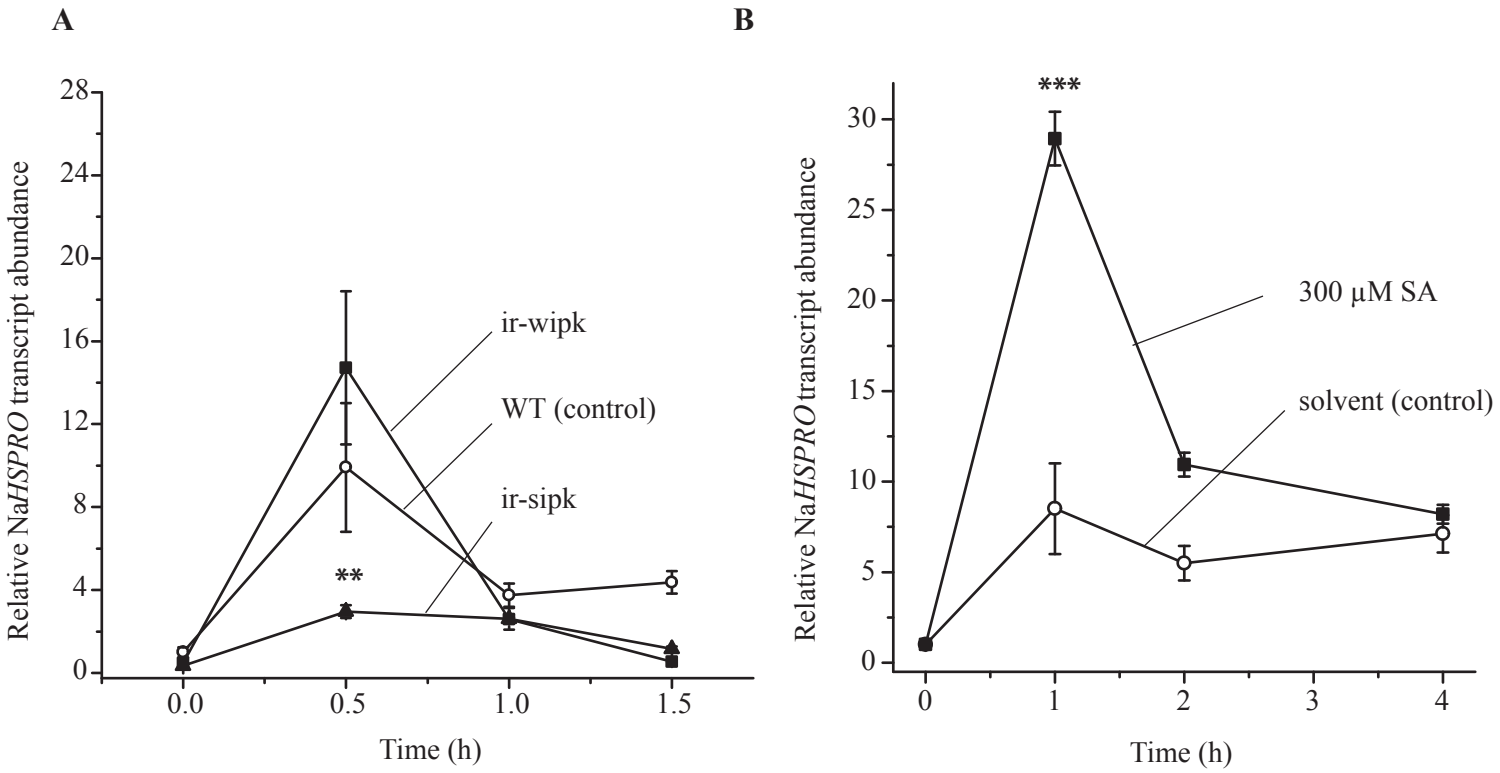

Supplemental Figure S3. Analysis of *HSPRO* expression in WT plants and in transgenic plants reduced in MAP kinase expression.

(a) Leaves of rosette-stage transgenic *N. attenuata* plants with reduced levels of SIPK (salicylic acid induced protein kinase) and WIPK (wound induced protein kinase) expression as well as control WT plants were elicited with synthetic 18:3-Glu. Total RNA was extracted from treated leaves at different times and *HSPRO* transcript levels were quantified by qPCR. *HSPRO* mRNA levels are expressed relative to the levels of the reference gene Na-*EF1A*. Quantification was performed by the ΔCt method (n=3; bars= ±S.E.). One way-ANOVA with Tukey post-hoc test (WT vs. ir-*sipk*); **: P<0.01. **(b)** Rosette stage WT plants were sprayed with 300 µM SA or control solution (see Materials and Methods for details). Leaves were harvested at different times and total RNA was extracted. *HSPRO* transcript levels were quantified as in (a) (n=3; bars= ±S.E.). Student's t-test (SA vs. control treatment); ***: P<0.001.

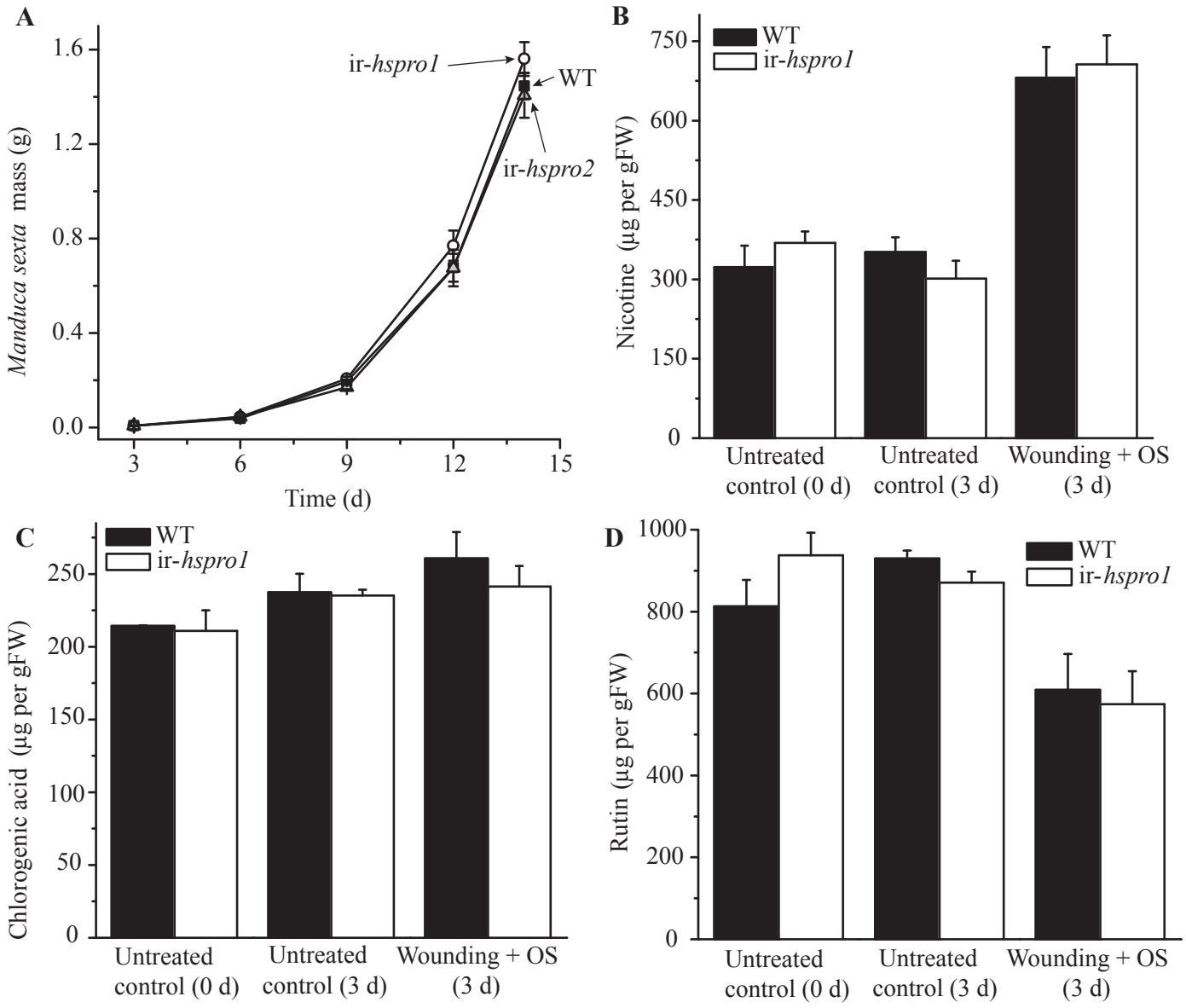

Supplemental Figure S4. Analysis of defense responses against *M. sexta* in WT and ir-*hspro* plants.

(a) Freshly hatched *M. sexta* neonates were placed on leaves of rosette stage *N. attenuata* WT and ir-*hspro* plants (one neonate per plant) and the caterpillar masses were quantified every 3 days for a period of 15 days (n=22 to 67; bars= ±S.E.). **(b,c,d)** Leaves from rosette stage WT and ir-*hspro1* plants were elicited with *M. sexta* OS once a day for three consecutive days. After three days (six days from the start of the treatment), leaves were harvested and used for quantification of defense metabolites by HPLC-UV. Control samples were leaves from untreated plants harvested either before the start of the treatment (0 days) or after three days (3 d) (n=5; bars= ±S.E.; (b) Nicotine; (c) Chlorogenic acid; (d) Rutin).

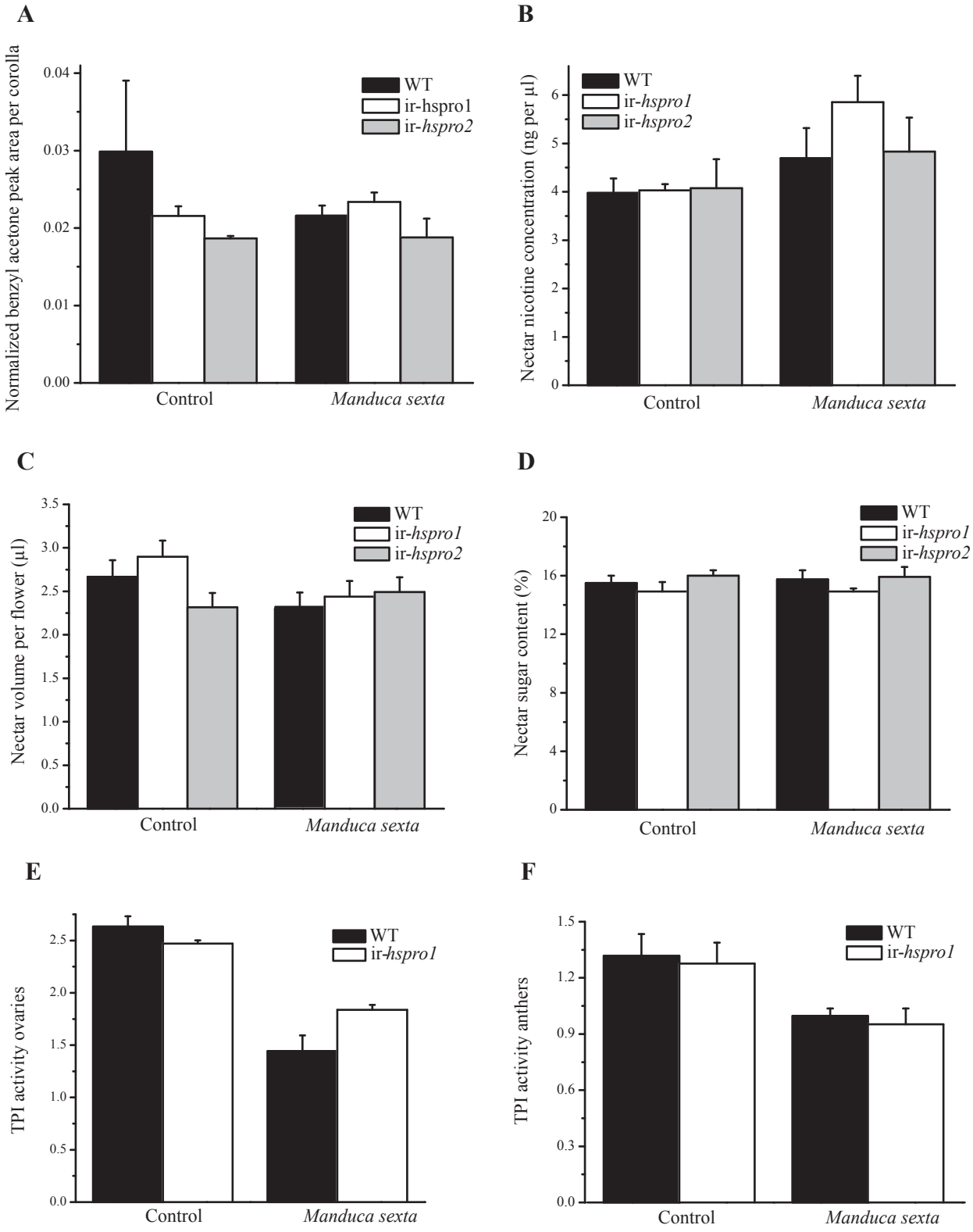

Supplemental Figure S5. Analysis of flower traits associated with the interactions of *N. attenuata* plants with insects.

N. attenuata WT and ir-*hspro* plants were challenged with *M. sexta* larvae for 15 consecutive days. Un-attacked plants were used as controls. **(a)** After removal of the caterpillars from the plants, 30 corollas from night opening flowers per genotype and treatment were collected. Samples consisting of 10 pooled corollas (*n*=3 per genotype per treatment) were extracted with dichloromethane and benzyl acetone levels were analyzed by GC-MS. Quantification was performed with tetraline as the internal standard. Bars denote S.E. **(b)** After removal of the caterpillars from the plants, the nectar from 10 individual flowers was pooled into a 1.5 mL tube to form one sample. The nectar volume was quantified with a glass capillary (*n*=3 [3x10 corollas]; bars= ±S.E.). **(c)** Nicotine levels in nectar collected in (b) were quantified by LC-MS using $^{2}H_{3}$-nicotine as internal standard (*n*=3; bars= ±S.E.). **(d)** Nectar collected in (b) was also used to determine sugar content with a refractometer (*n*=3; bars= ±S.E.). **(e,f)** After removal of the caterpillars from the plants, ovaries (e) and anthers (f) from 10 flowers were collected into a 1.5 mL tube to form one sample. Samples were used for protein extraction and measurement of trypsin proteinase inhibitor (TPI) activity (*n*=5; bars= ±S.E.).

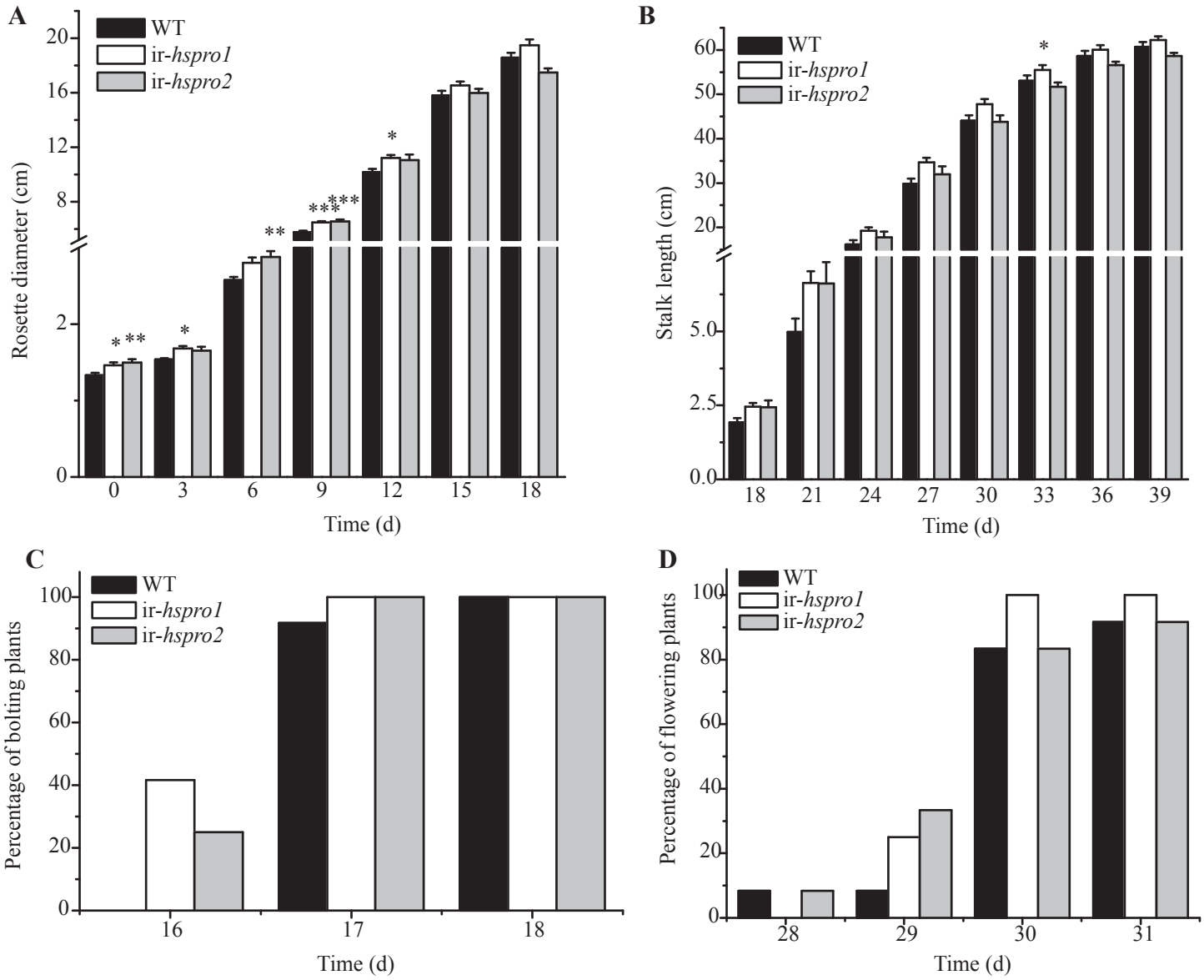

Supplemental Figure S6. Analysis of growth and developmental parameters of *P. indica*-colonized plants grown in the glasshouse.

WT and ir-*hspro* seedlings were grown on plates in the presence of *P. indica* for 14 days and the seedlings were then transferred to soil in 1L pots and grown in the glasshouse under standard growth conditions. **(a)** Rosette diameter (distance between the two longest leaves) and **(b)** stalk length were measured every three days. One way-ANOVA with Tukey post-hoc test (WT vs. ir-*hspro*); *: $P<0.05$; **: $P<0.01$; ***: $P<0.001$; $n=12$ per genotype (bars= ±S.E). **(c)** Bolting time (determined as the appearance of the reproductive meristem) and **(d)** flowering time (determined as the appearance of the first opened bud) were recorded daily ($n=12$ per genotype).

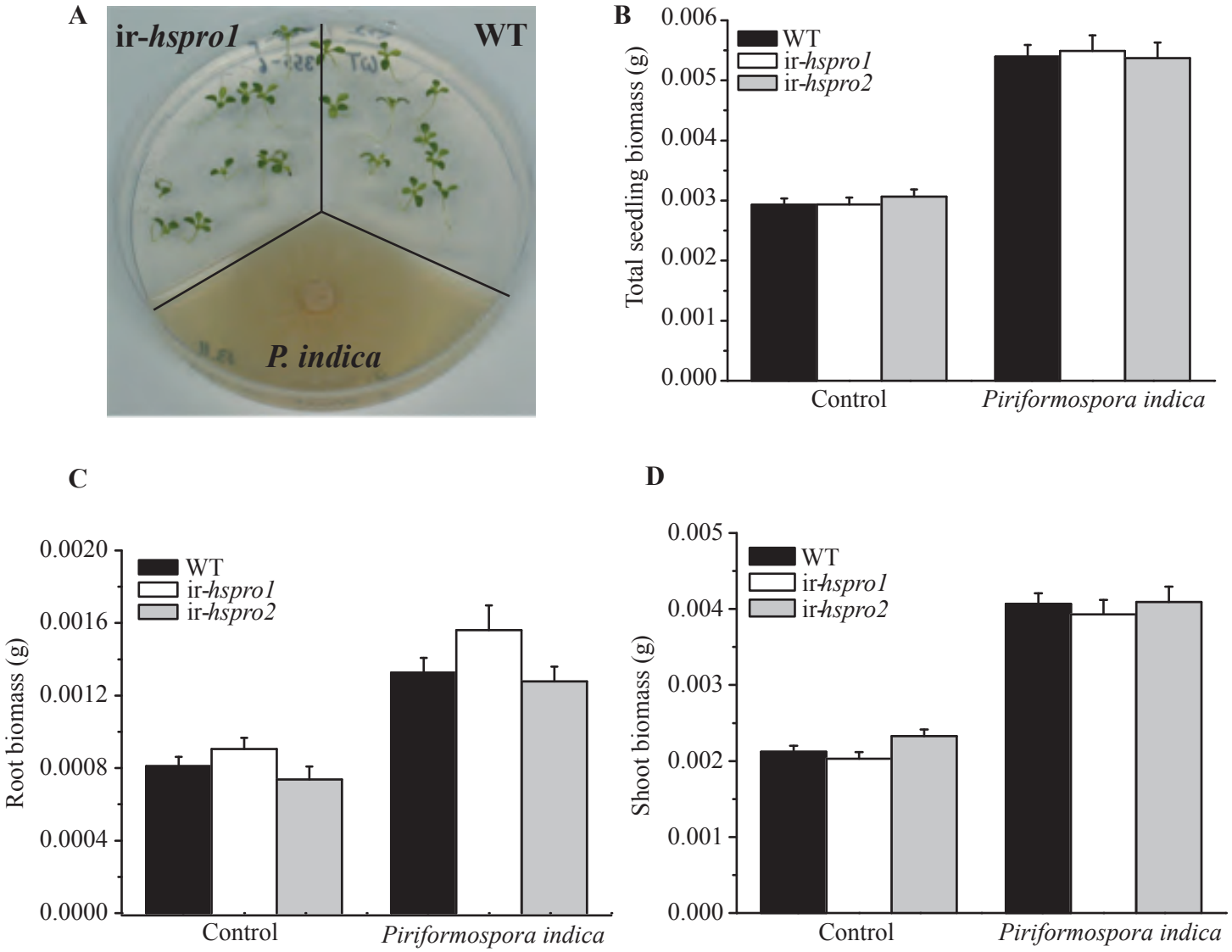

Supplemental Figure S7. Analysis of growth promotion of WT and ir-*hspro* seedlings induced by *P. indica* in a split-plate system.
(a) WT and ir-*hspro* seedlings and *P. indica* were grown in separate compartments of split Petri dishes (10 WT and 10 ir-*hspro* seedlings per plate) for 14 days. Plates without *P. indica* but with fungal media were used as controls. **(b,c,d)** Determination of fresh biomasses of total seedlings (b), shoots (c), and roots (d) was performed with a microbalance (n=26 to 29; bars= ±S.E.).

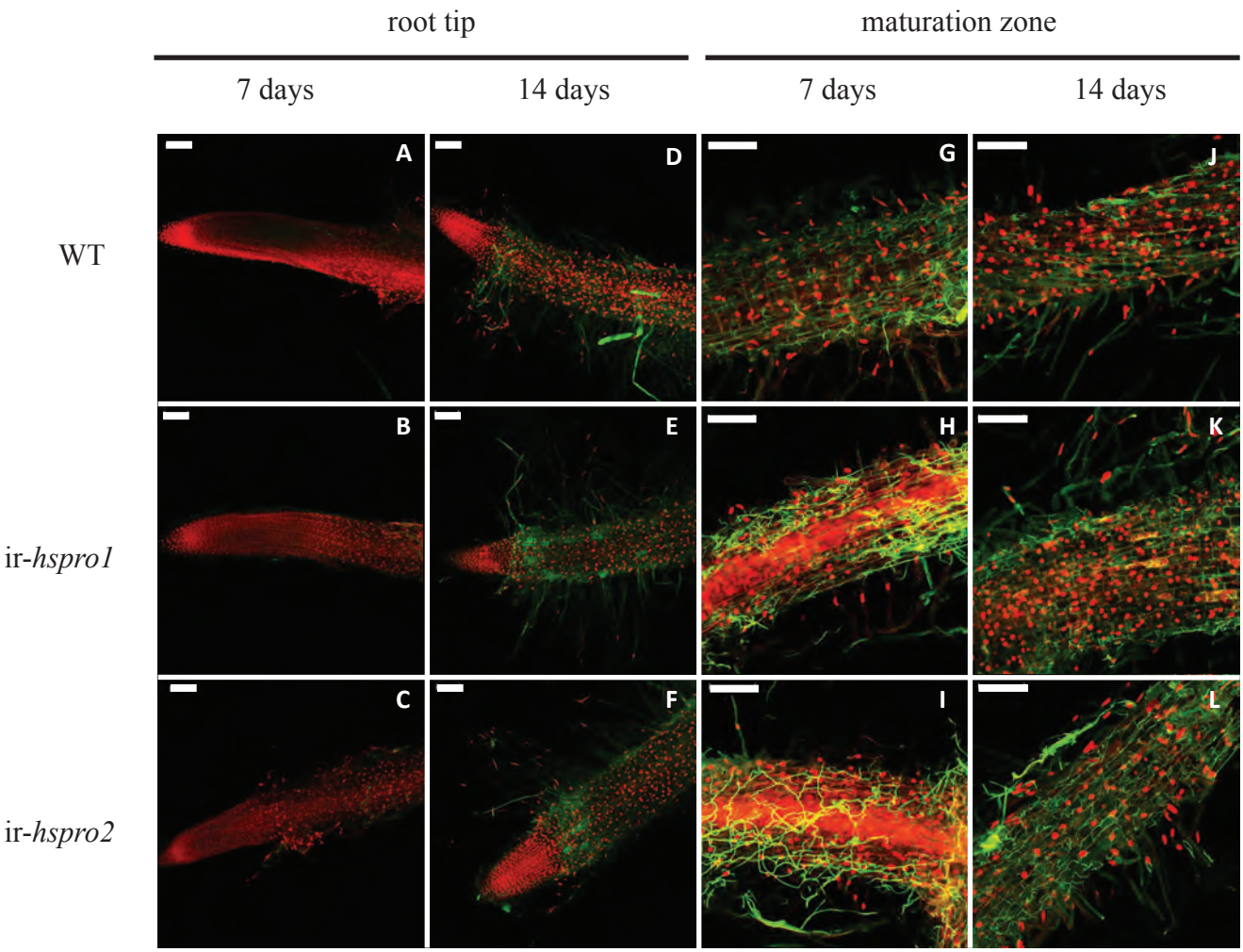

Suppl. Figure S8. Laser confocal microscopy analysis of roots from *P. indica*-colonized WT and ir-*hspro* seedlings.
(a-l) Root samples from seedlings grown in the presence of *P. indica* for 7 and 14 days were stained with WGA-AF488 (fungal structures; green) and propidium iodide (cell walls; red). Images were taken with a laser confocal microscope equipped with an argon laser. Excitation/detection was at 488/500-540 nm for WGA-AF488 and at 560/580-660 nm for propidium iodide. White bar: 100 µm.

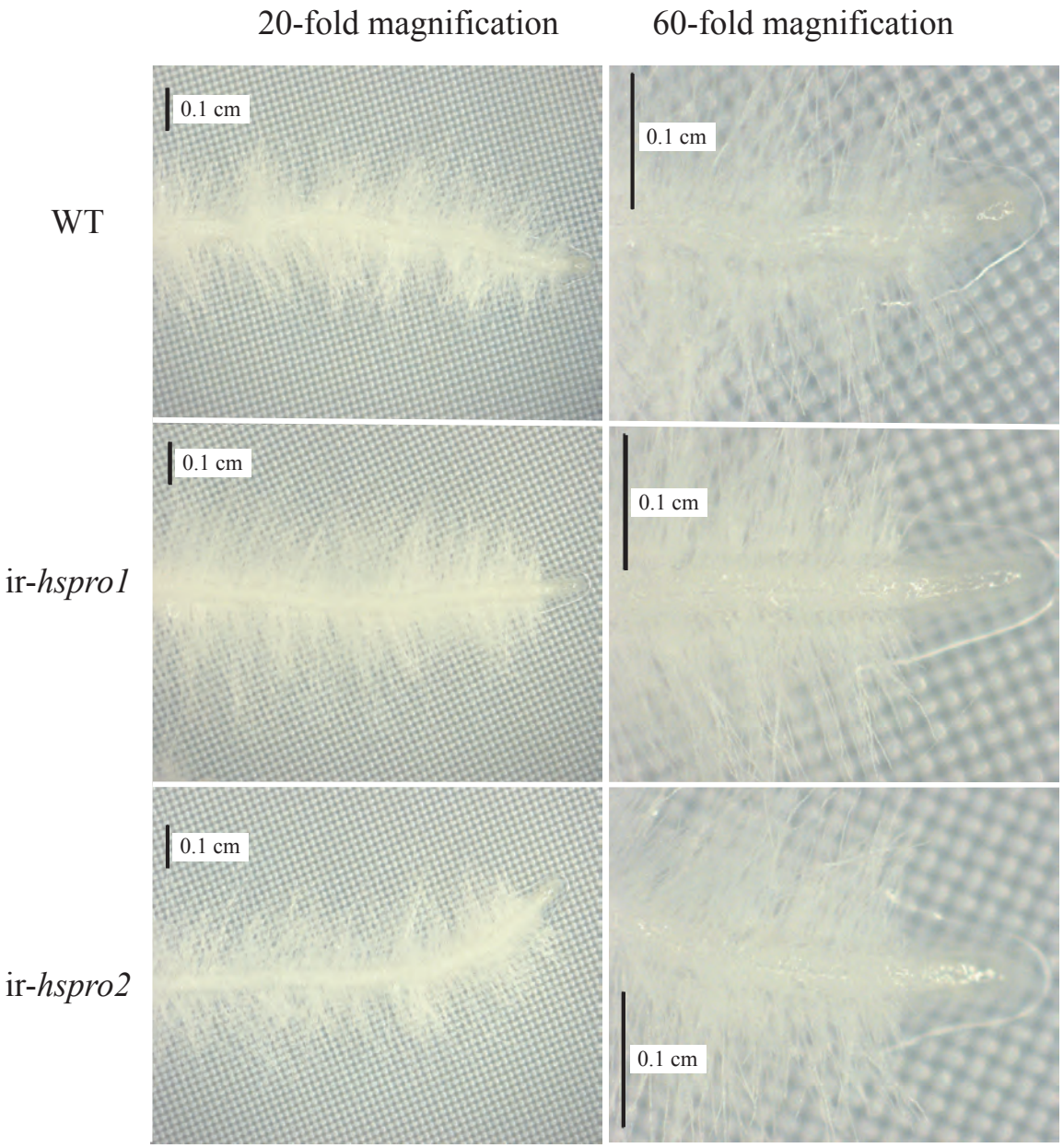

Supplemental Figure S9. Root morphology of *P. indica*-colonized WT and ir-*hspro* seedlings.
WT and ir-*hspro* seedlings were grown in the presence and absence of *P. indica* for 14 days on a plate system. Seedling roots were visualized under a stereomicroscope at 20- and 60-fold magnifications. Bars represent 0.1 cm.

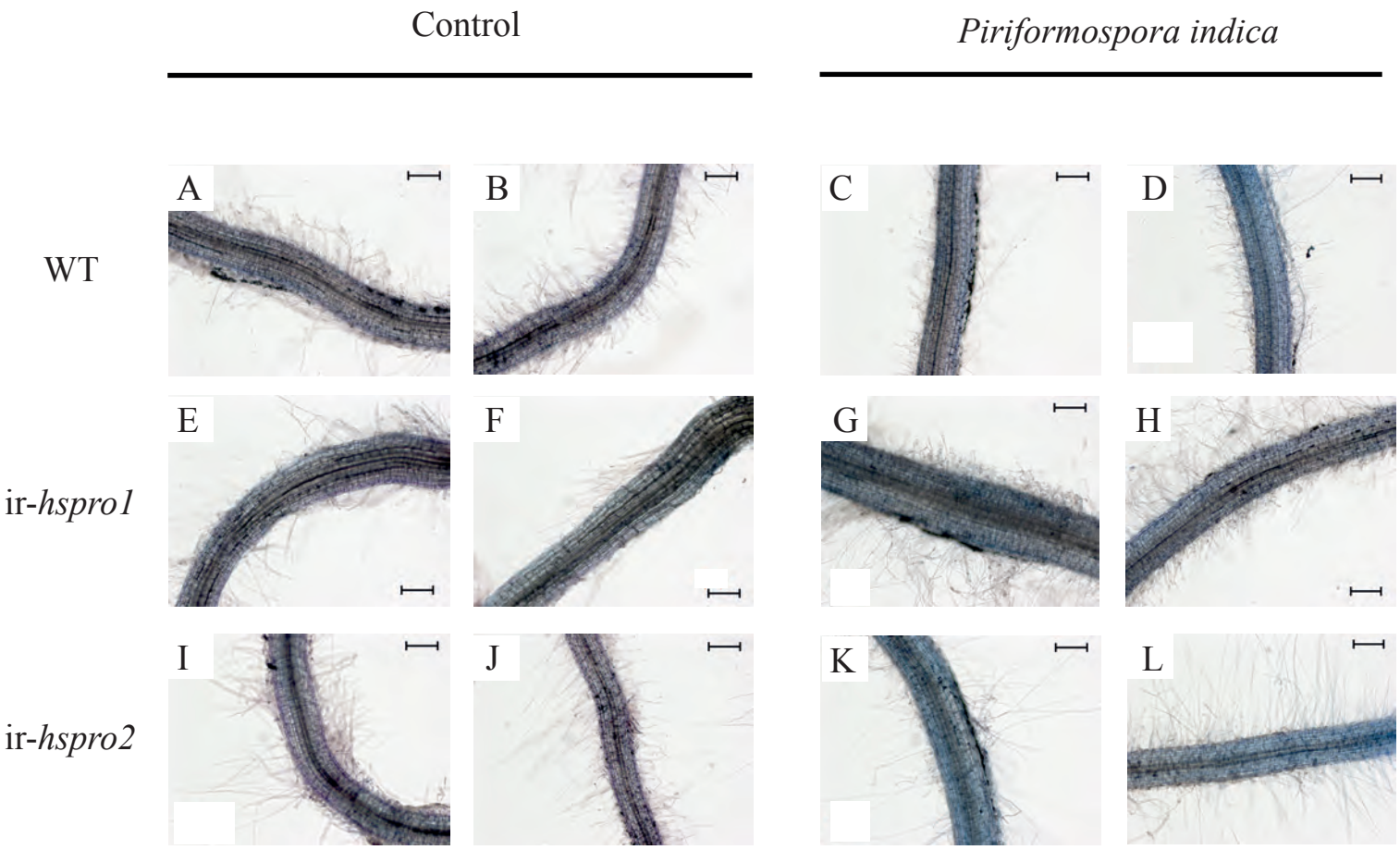

Figure S10. Analysis of root cell death in WT and ir-*hspro* seedlings.

WT and ir-*hspro* seedlings were grown in the absence (control) and presence of *P. indica* for 14 days on a plate system. Roots were excised from the seedlings and stained with trypan-blue. Images were taken with a Zeiss Imager.Z1 microscope using the AxioVision software. Bars represent 200 µm.

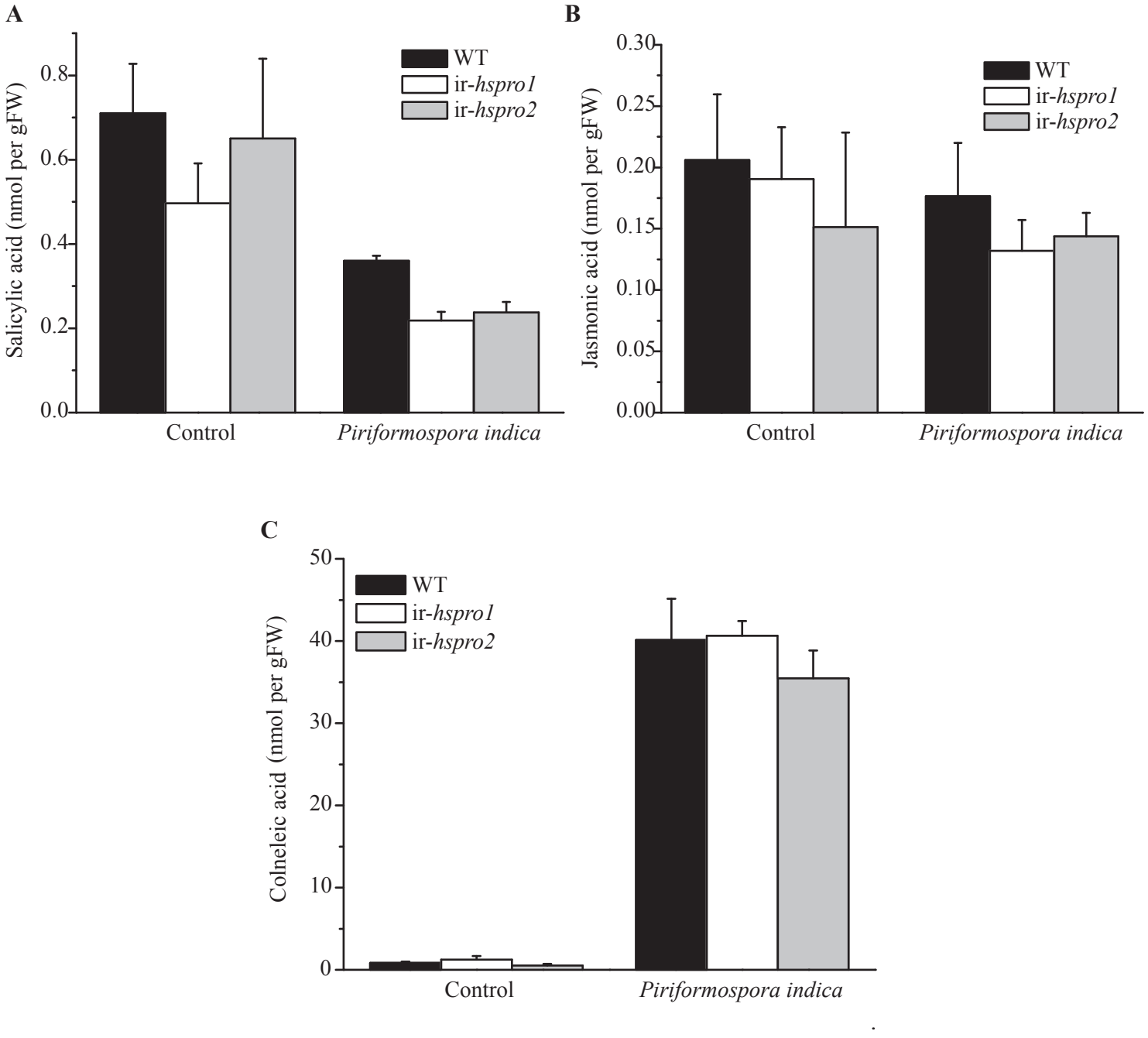

Supplemental Figure S11. Analysis of SA, JA and CA levels in roots of WT and ir-*hspro* seedlings. WT and ir-*hspro* seedlings were grown in the presence and absence of *P. indica* for 14 days on a plate system. Root samples were collected from the seedlings and the levels of **(a)** SA, **(b)** JA and **(c)** CA were quantified by LC-MS (n=3; bars= ±S.E.).

Supplemental Table SI. Analysis of WT and ir-*hspro* seedling's biomasses during *P. indica*-root colonization and control treatments.

Days of seedling growth	Genotype	Seedling weight (mg) ± SE [control]	*n*	Seedling weight (mg) ± SE [*P. indica*]	*n*	% growth promotion (*P.indica* vs. control)	% differential growth promotion (ir-hspro vs. WT)	*P*-value[1] (control vs. P. indica)	*P*-value[2] (WT vs. ir-hspro)
10	WT	14.2±0.9	16	30.4±1.6	20	**114**		6.33×10^{-13}	
	ir-hspro1	14.1±0.6	17	37.0±0.9	18	**162**	**42**	6.27×10^{-13}	3.62×10^{-3}
	ir-hspro2	13.8±0.4	15	41.2±0.2	18	**198**	**73**	6.27×10^{-13}	6.72×10^{-8}
	ir-hspro3	16.1±0.8	18	38.8±1.5	20	**140**	**23**	6.27×10^{-13}	2.70×10^{-5}
10	WT	20.8±2.1	20	28.6±1.8	20	**37**		0.03	
	ir-hspro1	22.8±1.7	18	35.6±1.8	18	**56**	**51**	6.13×10^{-5}	0.08
	ir-hspro2	20.9±2.0	20	32.4±1.3	20	**55**	**48**	1.62×10^{-4}	0.64
14	WT	14.5±0.8	12	28.6±1.0	17	**97**		5.77×10^{-13}	
	ir-hspro1	14.4±0.3	9	32.1±0.7	17	**123**	**26**	5.77×10^{-13}	0.02
	ir-hspro2	15.3±0.6	12	32.6±1.0	18	**113**	**17**	5.77×10^{-13}	4.08×10^{-3}
14	WT	13.2±0.9	10	39.6±1.9	24	**200**		1.97×10^{-12}	
	ir-hspro1	14.9±0.6	10	47.7±1.7	21	**220**	**10**	5.72×10^{-13}	3.51×10^{-3}
14	WT	13.5±0.7	10	38.9±1.9	11	**189**		6.27×10^{-13}	
	ir-hspro1	14.8±0.8	11	49.0±2.4	9	**231**	**22**	6.26×10^{-13}	2.05×10^{-4}
	ir-hspro2	14.7±0.4	7	47.8±1.5	6	**223**	**18**	6.26×10^{-13}	6.31×10^{-3}
14	WT	15.5±0.4	15	52.3±1.8	26	**245**		5.94×10^{-13}	
	ir-hspro1	14.4±0.6	20	60.1±1.7	22	**302**	**23**	5.94×10^{-13}	1.99×10^{-3}
	ir-hspro2	14.1±0.3	23	59.9±2.0	24	**302**	**23**	5.94×10^{-13}	1.93×10^{-3}
14	WT	11.5±0.3	9	37.2±2.5	30	**223**		1.73×10^{-6}	
	ir-hspro1	12.0±1.0	10	53.9±3.2	30	**349**	**56**	8.50×10^{-13}	5.41×10^{-4}
	ir-hspro2	13.4±0.9	10	47.9±2.6	30	**257**	**15**	1.38×10^{-10}	0.04

[1,2:] One way-ANOVA with Turkey post-hoc test (WT vs. ir-*hspro*).

Supplemental Table SIV. List of ions with differential accumulation in *P. indica*-colonized roots of ir-*hspro* compared to WT seedlings (positive mode of ionization).

Identity	log_2(FC[a])	*P*-value[b]	*m/z*	RT[s][c]	Mean peak intensity (ir-*hspro*)	S.E.	Mean peak intensity (WT)	S.E.
Unknown	-1.45	0.0348	381.789	437.273	131.929	81.947	400.507	61.602
Unknown	-1.12	0.0356	382.264	416.608	88.699	49.445	299.992	49.642
Unknown	-1.07	0.0376	450.199	165.750	77.202	43.625	272.628	50.775

[a]: FC: fold-change (ir-*hspro* vs WT)

[b]: *P*-value: Fisher´s t-test (ir-*hspro* vs WT); *n*=5

[c]: RT[s]: retention time (seconds).

Supplemental Table SV. List of primers.

Gene name	template	experiment	Forward 5'→3'	Reverse 5'→3'
Na*TEF1a*/ Na*tef1a*	cDNA/ gDNA	qRT-PCR	ACACTTCCCACATTGCTGTCA	AAACGACCCAATGGAGGGTAC
Na*HSPRO*	cDNA	qRT-PCR	CTGATCCTAGACCGTATGCGAACA	CTGACAACCGTCGTCTCATCAGA
Pi*tef1a*	gDNA	qRT-PCR	TCGTCGCTGTCAACAAGATG	GGATACAACCCCAAGACGGT
Na*HSPRO* (ORF)	cDNA	HSPRO- EGFP fusion product	ATGGTTGATTGCGATAGAAAGACAAAG ATGATATC	GGCCTTGTTACTTCTCTCTGGACTATACT TG
Na*HSPRO* (ORF + partial attB sequence)	PCR product	HSPRO- EGFP fusion product	AAAAAGCAGGCTATGGTTGATTGCGAT AG	AGAAAGCTGGGTTGGCCTTGTTACTTC
Na*HSPRO* (ORF + complete attB sequence)	PCR product	HSPRO- EGFP fusion product	GGGGACAAGTTTGTACAAAAAAGCAGG CT	GGGGACCACTTTGTACAAGAAAGCTGG GT
nptII	*nptII*-contai-ning plasmid	Probe (Southern-blot)	CCGGATCGGACGATTGCG	CGTCTGTCGAGAAGTTTCTG
At*RGA* (ORF + partial attB sequences)	cDNA	RGA-eGFP fusion product	AAAAAGCAGGCTTGAAGAGAGATCATC ACCAA	AGAAAGCTGGGTTGTACGCCGCCGTCG AGA
DCL2	gDNA	positivecontrol (diagno-stic PCR)	AAGGATGGCTCATTCCTGGTG	AGAGCTTCAACAAGCAGAGAAGG
Na*HSPRO* inverted repeat construct 5' end	gDNA	diagnostic PCR	GGAAGTTCATTTCATTTGGAG	CATACTAATTAACATCACTTAAC
Na*HSPRO* inverted repeat construct 3' end	gDNA	diagnostic PCR	GGTAACATGATAGATCATGTC	GCGAAACCCTATAGGAACCC
Na*HSPRO*	cDNA	3'-RACE	CTGATCCTAGACCGTATGCG	According to Invitrogen Kit
Na*HSPRO*	cDNA	3'-RACE	TCGAAAACCGAACGCTGTAC	According to Invitrogen Kit
Na*HSPRO*	cDNA	3'-RACE	CGACACACCAGATCCTCGAA	According to Invitrogen Kit
Na*HSPRO*	cDNA	5'-RACE	According to Invitrogen Kit	AAGCATTTTTGACGCGTAGATCC
Na*HSPRO*	cDNA	5'-RACE	According to Invitrogen Kit	GCACAACAGAGCTATG
Na*HSPRO*	cDNA	5'-RACE	According to Invitrogen Kit	TCCATCGCCAACGATTCAAGCCTC
Na*HSPRO*	cDNA	Generation of ir-hspro construct	GTCGACACGACGGTTGTCAGCCAGAC	GGATCCGTAGATCCATGTTTCGAGGATC

Supplemental Experimental Procedures S1

Full length cDNA cloning, EGFP fusion protein generation, and sequence analysis

For the cloning of the full length *HSPRO* cDNA sequence, 5 µg of total RNA were isolated from leaves of *N. attenuata* plants. The 3´RACE and 5'RACE Systems for Rapid Amplification of cDNA Ends (Invitrogen, Karlsruhe, Germany) were used following the manufacturer's instructions and the primers listed in Supplemental Table SV. The PCR products were cloned into the pGEM-T easy vector (Promega, Madison, WI) and sequenced using universal primers. Sequence alignments and phylogeny analysis were performed using BLAST (http://blast.ncbi.nlm.nih.gov) and the Geneious Pro software (version 5.4; Drummond *et al.*, 2011). Phylogenetic analysis was performed with the Jukes-Cantor genetic distance model and the Neighbor Joining tree building method with bootstrapping (602 random seed, 100 replicates and 50% support threshold).

To generate C-terminal EGFP fusion proteins, the HSPRO protein coding sequence was amplified by PCR from *N. attenuata* cDNA and the nuclear localized DELLA protein RGA (Silverstone *et al.*, 2001) was amplified from Arabidopsis Col-0 cDNA (primers listed in Supplemental Table SV). PCR products were cloned into the pJET1.2 vector (Fermentas, East Lansing, MI) and transformed into *E. coli* TOP10 strain by electroporation using standard conditions. The Gateway vector pDONR221 (Invitrogen) was used as the entry vector and p2GWF7 (Karimi *et al.*, 2007) as the destination vector for C-terminal fusions to EGFP. Leaf Arabidopsis protoplasts were isolated and transformed by the polyethylene glycol (PEG) method as previously described (Yoo *et al.*, 2007). Protoplasts were incubated for 15 h in the dark at room temperature before visualization with a Zeiss Axioplan fluorescence microscope (Carl Zeiss, Jena, Germany) using standard settings for EGFP.

Genomic DNA extraction for qPCR analysis of *P. indica* root colonization

Genomic DNA from *N. attenuata* seedlings was extracted with 2 mL of extraction buffer (2 % (w/v) CTAB, 100 mM Tris-HCl pH:8.0, 20 mM EDTA, 1.4 M NaCl, 2 % (w/v) polyvinylpyrrolidone and 0.5% (v/v) 2-mercaptoethanol) pre-heated to 65ºC. Samples were kept at 65ºC for 1 h and repeatedly mixed by inverting the tube. After centrifugation (8,000 *g* for 5 min), the supernatant was collected and transferred into 50 mL plastic tubes. This initial extraction step was repeated twice. The pooled supernatants were extracted twice with 1/3 volumes (~0.6 mL) of chloroform:isoamyl alcohol (24:1) by continuously inverting the tube for 10 min and centrifugation (8,000 *g* for 10 min). 0.1 volumes (~60 µL) of 10% (w/v)

CTAB solution were added to the sample and after mixing by inverting the tube, 1.4 volumes (~1 mL) of precipitation buffer (1% (w/v) CTAB, 50 mM Tris-HCl pH=8.0, 10 mM EDTA) were added and mixed gently. After an overnight incubation, the tubes were centrifuged at 4,500 *g* for 15 min. The supernatant was removed and the pellet dissolved in 500 µL of high-salt TE (10 mM Tris-HCl pH=8.0, 0.1 mM EDTA, 1 M NaCl) containing 0.5 µg mL^{-1} RNAse-A for 20 min at 37ºC. The genomic DNA was precipitated by mixing the sample with 1 volume (500 µL) of isopropanol and incubating the mixture for 30 min. The samples were centrifuged at 16,100 *g* for 30 min and the pellet was washed with 500 µL of 70% (v/v) ethanol and finally dissolved in 5 µL of deionized water. The genomic DNA concentration was estimated by absorbance and by comparing the signal intensities on a 0.8% (w/) agarose gel to the intensities of a DNA ladder standard of known concentration.

Quantification of defense and flower-associated traits

In the morning (6 to 8 am), the nectar from 10 flowers was collected and pooled into a 1.5 mL tube to form one sample. The nectar volume per sample was determined with a graduated glass capillary. Nectar sugar content was measured with a refractometer using a sucrose standard curve. Nectar nicotine was quantified by LC-MS (liquid chromatography-mass spectrometry; Varian 1200 Triple-Quadrupole-LC-MS system; Varian, Palo Alto, CA) (see below) from samples containing 2 µL of nectar dissolved in 400 µL of deionized water spiked with 50 pg [$^2H_3$]nicotine.

For analysis of benzyl acetone (BA) in corollas, 10 corollas from recently opened (10 to 12 pm) night flowers were pooled per sample. The samples were frozen in liquid nitrogen and homogenized in 15 mL glass vials after adding 2 mL dichloromethane containing 2 µg tetraline mL^{-1}. Corolla tissue was spun down by centrifugation at 720 *g* for 10 min at room temperature. The supernatant was transferred into new glass vials with a Pasteur pipette and washed by adding 2 mL of deionized water. An aliquot from the organic phase was transferred into a glass vial and analyzed by GC-MS with a CP-3800 GC instrument (Varian 4000) equipped with a DB-Wax column (Agilent) as previously described (Re *et al.*, 2011). For identification of the benzyl acetone peak, the retention time and mass spectra were compared to a commercial standard (Sigma). Three biological replicates were used per genotype and treatment.

TPI activity from anthers and ovaries was quantified as previously described (Van Dam *et al.*, 2001). Anthers and ovaries from 10 flowers were pooled per sample and 5 samples were analyzed per genotype and treatment. Quantification of nicotine, rutin, and

chlorogenic acid after *M. sexta* OS elicitation of leaves was performed as previously described (Keinänen *et al.*, 2001). Leaves of rosette-stage plants were elicited by wounding and *M. sexta* OS elicitation once per day for three consecutive days and leaf samples were harvested at the end of the third day (six days after the start of the treatment).

Phytohormone and divinyl ether extraction and quantification

One hundred mg of *P. indica*-colonized roots (from seedlings grown for 14 days in the plate system) were homogenized to a fine powder with a Geno/Grinder 2000 (BTC and OPS Diagnostics, Bridgewater, USA) in the presence of liquid nitrogen. Each sample (biological replicate) consisted of roots pooled from 6 to 11 seedlings and 3 biological replicates per genotype per treatment were used. One mL of ethyl acetate spiked with 200 ng [$^2H_2$]JA, [$^2H_4$]SA, and [$^2H_6$]ABA as IS was used for extraction. The samples were centrifuged for 15 min at 12,000 *g* (4°C) and the upper organic phase was transferred into a fresh tube. The residual leaf material/aqueous phase was re-extracted with 0.5 mL ethyl acetate without IS. The organic phases were pooled and evaporated to dryness under reduced pressure. The dry residue was reconstituted in 0.4 mL of 70/30 (v/v) methanol/water for analysis by LC-MS (Varian 1200) as previously described (Bonaventure *et al.*, 2011).

For the analysis of ET, seedlings from WT and ir-*hspro* plants were weighed and transferred into a 250 mL glass vessel. Ten seedlings were placed in each glass vessel and a total of three glass vessels (n=3) were used per genotype. After a 5 h incubation period (glass vessels were kept in the growth chamber under the same conditions as the agar plates), the headspace of the vessels was flushed into a laser photo-acoustic spectrometer (PAS; INVIVO, Adelzhausen, Germany) for determination of ET levels (nL $h^{-1}g^{-1}$ FW) as previously described (Körner *et al.*, 2009).

Metabolic profiling of roots

P. indica-colonized roots from ir-*hspro* and WT seedlings (grown for 14 days in the plate system) were collected for metabolic profiling. Ten roots were pooled per sample and 5 samples (biological replicates) per genotype were used. Root tissue was ground with a Geno/Grinder 2000 in the presence of liquid nitrogen and thoroughly extracted with 1 mL of 40% (v/v) methanol/50 mM aqueous sodium acetate buffer (pH: 4.8) per 100 mg of root tissue. Homogenized samples were centrifuged at 12,000 *g* for 20 min at 4°C, the supernatant was transferred into a fresh 1.5 mL microcentrifuge tube and the samples were centrifuged again using the same conditions. 100 µL of the supernatant were transferred into 2 mL glass

vials for analysis by UPLC-ToF-MS (ultra-pressure-liquid-chromatography time-of-flight mass spectrometry; Bruker Daltonik GmbH, Bremen, Germany) as previously described (Gilardoni *et al.*, 2011).

Microarray analysis

P. indica-colonized roots from ir-*hspro* and WT seedlings (grown for 14 days in the plate system) were collected for microarray analysis. Ten roots were pooled per sample and 3 samples (biological replicates) per genotype were used. Total RNA was extracted as previously described (Kistner and Matamoros, 2005) and RNA quality was checked by spectrophotometry (NanoDrop, Wilmington, DE). Genomic DNA was removed by DNAse treatment following commercial instructions (Turbo DNase; Ambion, Europe), RNA was cleaned up with RNeasy MinElute columns (Qiagen, Hilden, Germany) and the RNA quality was checked with the RNA 6000 Nano kit (Agilent, Santa Clara, CA) using an Agilent 2100 Bioanalyzer. Total RNA was used to generate labeled cRNA with the Quick Amp labeling kit (Agilent) following commercial specifications and the yield of cRNA was determined spectrophotometrically (NanoDrop). Labeled cRNA was hybridized using the Gene Expression Hybridization kit (Agilent) following commercial instructions onto a 44K custom designed 60mer *N. attenuata* Agilent microarrays as previously described (Gilardoni *et al.*, 2011; Kallenbach *et al.*, 2011). Hybridization, washing and analysis were performed as previously described (Gilardoni *et al.*, 2011; Kallenbach *et al.*, 2011). Three biological replicates were used per treatment with a total of six arrays (see Accession numbers). Data was extracted using the Agilent Feature Extraction software (version 9.5) and analyzed with the SAM (Significance Analysis of Microarrays) software (Tusher *et al.*, 2001). The *q*-values for each gene corresponded to a computed false discovery rate (FDR) of less than 4%. Changes in gene expression were considered to be significant when the Log_2 of the fold change in signal intensity (ir-*hspro* versus WT) were greater than 1 or smaller than -1.

Root and fungus staining

Root samples from seedlings grown in the presence of *P. indica* for 7 and 14 days were fixed in 0.15 % (w/v) trichloroacetic acid in 4:1 (v/v) ethanol/chloroform as previously described (Deshmukh *et al.*, 2006). Samples were stained with WGA-AF488 (fungal structures; green) and propidium iodide (cell walls; red) as previously described (Zuccaro *et al.*, 2011). Confocal laser scanning microscopy was performed using a LSM 510 Meta microscope (Carl Zeiss) equipped with an argon laser. Samples were excited at 488 nm and

light emission detected at 500-540 nm for WGA-AF488. For propidium iodide, samples were excited at 560 nm and light emission detected at 580-660 nm. Macroscopic observations of WT and ir-*hspro* seedling roots grown for 14 days on the plate system in the presence or absence of *P. indica* was carried out with a stereomicroscope (Olympus SZ51). Cell death analysis in roots was performed by trypan-blue staining as previously described (Diaz-Tielas *et al*., 2012)

M. sexta performance assays and OS collection

Larvae of the tobacco hornworm (*Manduca sexta*) were obtained from in-house colonies, generated from *M. sexta* eggs originally purchased from the Carolina Biological Supply (North Carolina, US). Eggs deposited on *N. attenuata* plants were collected and were kept in a growth chamber (Snijders Scientific) at 26°C/16 h day and 24°C/8 h night until the larvae hatched. *M. sexta* and *Spodoptera exigua* OS was collected as described by (Roda *et al.*, 2004). For *M. sexta* larval growth performance assay, freshly hatched neonates were placed carefully on leaves of rosette-stage *N. attenuata* plants (one neonate per plant). A minimum of 30 plants per genotype were used. Caterpillars were weighed every two to three days for two weeks.

References

Bonaventure G, Schuck S, Baldwin IT (2011) Revealing complexity and specificity in the activation of lipase-mediated oxylipin biosynthesis: a specific role of the Nicotiana attenuata GLA1 lipase in the activation of jasmonic acid biosynthesis in leaves and roots. Plant Cell Environ **34:** 1507-1520

Deshmukh S, Huckelhoven R, Schafer P, Imani J, Sharma M, Weiss M, Waller F, Kogel KH (2006) The root endophytic fungus Piriformospora indica requires host cell death for proliferation during mutualistic symbiosis with barley. Proc Natl Acad Sci USA **103:** 18450-18457

Diaz-Tielas C, Grana E, Sotelo T, Reigosa MJ, Sanchez-Moreiras AM (2012) The natural compound trans-chalcone induces programmed cell death in Arabidopsis thaliana roots. Plant Cell Environ

Gilardoni PA, Hettenhausen C, Baldwin IT, Bonaventure G (2011) Nicotiana attenuata LECTIN RECEPTOR KINASE1 suppresses the insect-mediated inhibition of induced defense responses during Manduca sexta herbivory. Plant Cell **23:** 3512-3532

Kallenbach M, Gilardoni PA, Allmann S, Baldwin IT, Bonaventure G (2011) C(12) derivatives of the hydroperoxide lyase pathway are produced by product recycling through lipoxygenase-2 in Nicotiana attenuata leaves. New Phytol **191:** 1054-1068

Karimi M, Depicker A, Hilson P (2007) Recombinational cloning with plant gateway vectors. Plant Physiol **145:** 1144-1154

Keinänen M, Oldham NJ, Baldwin IT (2001) Rapid HPLC screening of jasmonate-induced increases in tobacco alkaloids, phenolics, and diterpene glycosides in Nicotiana attenuata. Journal of Agricultural and Food Chemistry **49:** 3553-3558

Kistner C, Matamoros M (2005) RNA isolation using phase extraction and LiCl precipitation. *In* A Márquez, ed, Lotus japonicus Handbook. Springer Netherlands, pp 123-124

Körner E, von Dahl C, Bonaventure G, Baldwin IT (2009) Pectin methylesterase NaPME1 contributes to the emission of methanol during insect herbivory and to the elicitation of defence responses in *Nicotiana*. J Exp Bot **60:** 2631-2640

Re DA, Dezar CA, Chan RL, Baldwin IT, Bonaventure G (2011) Nicotiana attenuata NaHD20 plays a role in leaf ABA accumulation during water stress, benzylacetone emission from flowers, and the timing of bolting and flower transitions. J Exp Bot **62:** 155-166

Roda A, Halitschke R, Steppuhn A, Baldwin IT (2004) Individual variability in herbivore-specific elicitors from the plant's perspective. Mol Ecol **13:** 2421-2433

Silverstone AL, Jung HS, Dill A, Kawaide H, Kamiya Y, Sun TP (2001) Repressing a repressor: gibberellin-induced rapid reduction of the RGA protein in Arabidopsis. Plant Cell **13:** 1555-1566

Tusher VG, Tibshirani R, Chu G (2001) Significance analysis of microarrays applied to the ionizing radiation response. Proc Natl Acad Sci U S A **98:** 5116-5121

Van Dam NM, Horn M, Mares M, Baldwin IT (2001) Ontogeny constrains systemic protease inhibitor response in Nicotiana attenuata. J Chem Ecol **27:** 547-568

Yoo S-D, Cho Y-H, Sheen J (2007) Arabidopsis mesophyll protoplasts: a versatile cell system for transient gene expression analysis. Nat. Protocols **2:** 1565-1572

Zuccaro A, Lahrmann U, Guldener U, Langen G, Pfiffi S, Biedenkopf D, Wong P, Samans B, Grimm C, Basiewicz M, Murat C, Martin F, Kogel KH (2011) Endophytic life strategies decoded by genome and transcriptome analyses of the mutualistic root symbiont Piriformospora indica. PLoS Pathog **7:** e1002290